AUSTRALIA

BMR RESEARCH NEWSLETTER

Number 13

ISSN 0813 - 751X

October 1990

Triassic and Jurassic carbonate buildups on the Exmouth Plateau

Are they petroleum prospects?

In 1988, Ocean Drilling Program (ODP) Leg 122 cored 200 m of Rhaetian reef complex at Site 764 on the Wombat Plateau north of the Exmouth Plateau (Fig. 1), overlying a Carnian–Norian deltaic complex (Mungaroo Formation) with some shelf carbonates (Williamson & others, 1989: *The APEA Journal*, 29.1; Haq & others, 1990: *Proceedings of the Ocean Drilling Program*, Vol. 122, *Initial Reports*). This was the first discovery of a Triassic reef in Australia, although Triassic and Jurassic shelf carbonates have been known for some time in the Exmouth Plateau region (von Rad & others, 1990: *BMR Journal of Australian Geology & Geophysics*, 11.4). It has led to the conclusion that Late Triassic and Early Jurassic reefs are potential petroleum reservoirs along much of the outer Northwest Shelf. Major reef complexes might also contain oil-prone source rocks, in contrast to the generally gas-prone Triassic sequences. Some evidence of a possible Jurassic reef is visible on a seismic section from near Mermaid Reef in the outer Canning Basin (Falvey & others, 1990: *The APEA Journal*, 30.1).

As a consequence of the ODP results, BMR's RV *Rig Seismic* was deployed in May this year to the northern Exmouth Plateau and outer Canning Basin in order to map reef complexes and to trace them, if possible, back into shallower water. Constituting BMR Survey 95, this cruise consisted of regional seismic profiles to tie exploration wells across the continental margin to the abyssal plain, a high-resolution seismic survey of the drilled reef complex on the Wombat Plateau, and a dredging program along the outer Canning Basin to substantiate regional seismic interpretations. The dredging showed that Triassic to Jurassic shallow-marine carbonates with shelly faunas are common along the Canning Basin margin, and include algal and coral boundstone. The dredge results will be reported fully in due course.

The reflection seismic survey of the Wombat Plateau, near ODP Sites 761 and 764, used a watergun array and a 96-channel, 1200-m-long seismic cable to record 255 km of high-resolution seismic data. The area surveyed (Fig. 1) lies in water 2000–3000 m deep and covers a rectangle about 30 x 20 km in size, with a line spacing of 2 km. The unprocessed monitor records indicate that reefs are more widespread in the north and that lagoonal sediments prevail in the south, in agreement with the ODP results. Processed north–south profile BMR 95/22, through ODP Site 764 (Fig. 2), clearly shows the drilled reef, and a number of other small reefs whose density of distribution decreases southward. The reefs on this seismic line are confined to the Rhaetian sequence, but on other lines they appear to extend into the

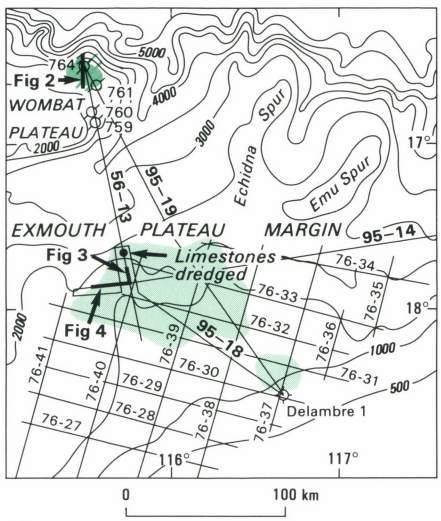

Fig. 1. Locations of selected seismic lines, ODP drill sites, and illustrated seismic profiles (Figs. 2–4), and distribution of Triassic and Jurassic buildups.

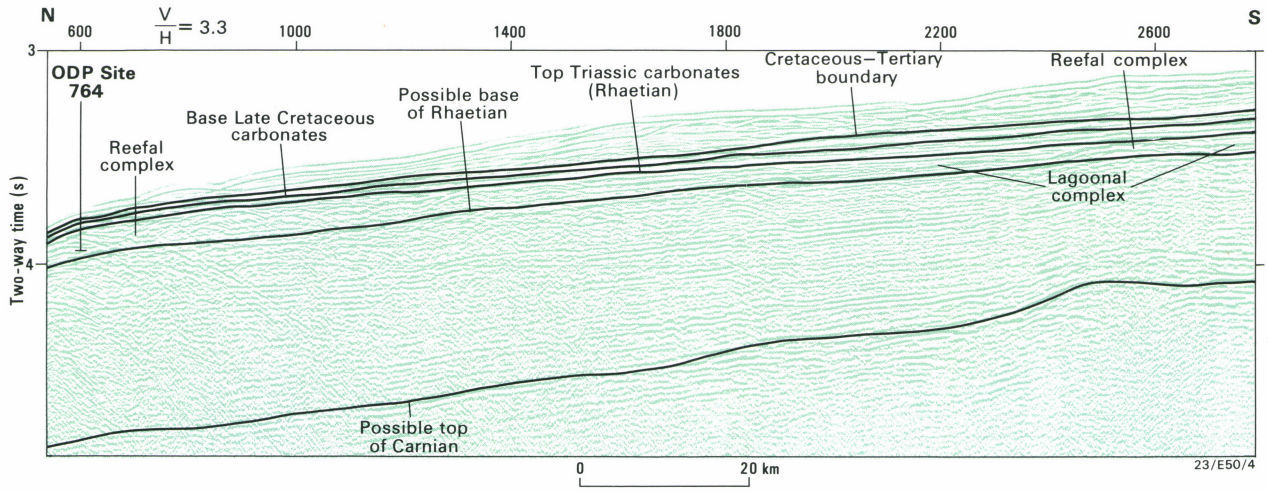

Fig. 2. High-resolution reflection seismic profile BMR 95/22, showing Rhaetian reefs on the Wombat Plateau (including that drilled at ODP Site 764).

Features of this issue

Published twice-yearly by the Australian Government Publishing Service for the

Bureau of Mineral Resources, Geology and Geophysics, Canberra

Department of Primary Industries and Energy

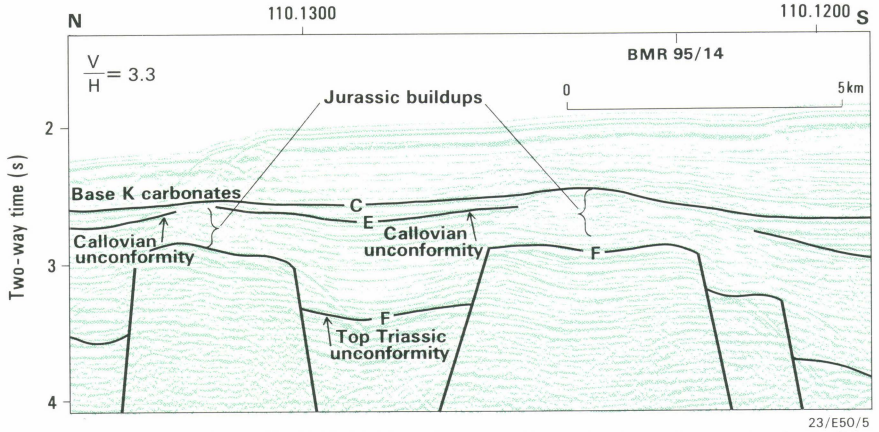

Fig. 3. Reflection seismic profile BMR 56/13 — shot normal to regional structure — showing buildups, believed to be Jurassic reefs according to geophysical and dredging evidence, on Triassic horst blocks.

Norian. Most of the reefs are of small to moderate size, but in some areas they amalgamate to form larger complexes.

During the planning of the regional seismic survey on the northern Exmouth Plateau south of the Wombat Plateau, numerous sedimentary buildups were identified on top of Triassic horst blocks on existing seismic profiles. Typical examples are on BMR seismic line 56-13 (Fig. 3), aligned roughly normal to the regional structure. The buildups lie on, but do not completely cover Triassic horst blocks, and are about 2 km across and 0.4 s (twt) thick. They are onlapped by the Oxfordian-Callovian E reflector and overlapped by the Upper Cretaceous C reflector, suggesting that they first formed in the Early Jurassic, were topographic highs for a long time, and were resistant to marine erosion (open-marine conditions developed in the Early Cretaceous).

During the survey, additional lines were placed to determine whether these buildups could be mapped over a substantial area, and that proved to be the case. Adjacent lines suggest that large horst blocks are frequently overlain by post-Triassic buildups that are 1-3 km wide and appear to extend along strike for 10-15 km. BMR profile 95-14, aligned virtually parallel to strike where it cuts BMR profile 56-13, shows a continuous buildup nearly 15 km long and up to 0.4 s thick (Fig. 4). Figure 3 and two adjacent Survey 95 profiles show that the buildup averages 2 km wide. If its velocity is 2000 m s^{-1}, its average thickness is around 300 m.

Similar buildups are widespread in other data sets, such as the GSI WAS-76 survey, and are plotted in Figure 1. They extend almost as far south as Delambre No. 1 well and into water depths a little less than 1000 m. The question is whether these Jurassic buildups are reefs like the Triassic ones; they might be instead volcanic flows or sills, or mounds of Jurassic siliciclastic or marly rocks. However, because they are seismically transparent and are seen only on the horst — not along faults or spreading into the grabens — we do not believe that they are igneous bodies. If they are shallow-marine Jurassic detrital accumulations, they would have been part of a thick Early Jurassic sedimentary blanket that was disrupted by fault movements associated with rifting. Once uplifted they would have been eroded to take up their present configuration. We consider that this is unlikely, because not only are these buildups generally more poorly bedded than the Jurassic sedimentary rocks in the grabens — and thus cannot have been juxtaposed during deposition — but they also had to survive as islands in the Early Cretaceous ocean, suggesting that they are more resistant than the Jurassic mudstone and marlstone known from wells in this area.

Follow-up dredging, on BMR Survey 96 in September 1990, has recovered hard ironstained mollusc-rich skeletal limestone and limestone breccia from an outcropping buildup along BMR seismic line 56-13 at latitude 17°38'S, longitude 115°42'E, below a water depth of 2250-1950 m, 15 km north of Figure 3.

Our conclusion is that the Jurassic buildups are almost certainly reefal complexes, like the Rhaetian one at ODP Site 764. They formed on the highs provided by Triassic horsts. They have never carried much overburden on the northernmost Exmouth Plateau — and hence retain their porosity — and are of low velocity, displaying no velocity pull-up under them. If they are reefal complexes, they may well be suitable targets for petroleum search in the right setting. Source rocks for Triassic or Jurassic reefal complexes could be Triassic shales (gas-prone), Jurassic shales (oil or gas prone), or lagoonal carbonates (oil prone). Overlying seals might be provided by Cretaceous mudstone, marlstone, or chalk. We still have to process all our data, but would encourage petroleum exploration companies to examine seismic profiles in outer Northwest Shelf leases for evidence of similar Triassic or Jurassic bodies.

For further information, contact Neville Exon, Doug Ramsay, or Barry West at BMR.

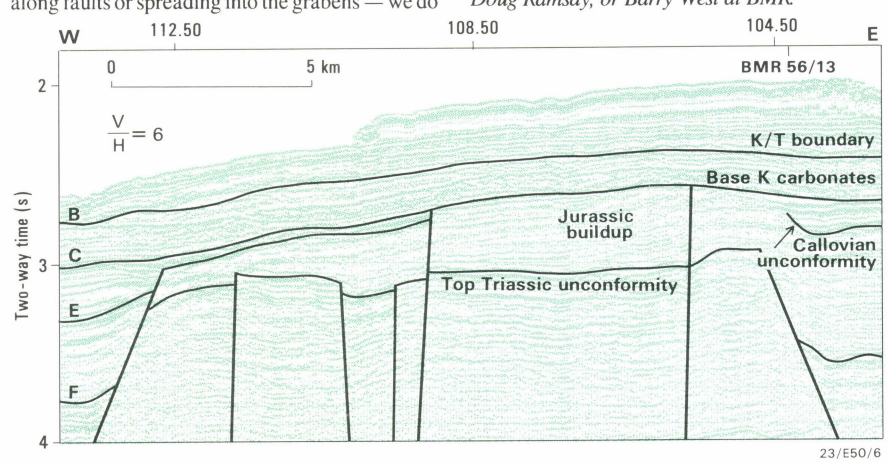

Fig. 4. Reflection seismic profile BMR 95/14 — shot normal to BMR 56/13 — which cuts the southern buildup on BMR 56/13 (Fig. 3) and shows it to be very extensive along strike.

Kosciusko geological map heralds new parks mapping project

In spite of a growing community interest in the landscapes of our wilderness areas, there is relatively little information readily available to the public on the rocks which form the foundation of those areas. The geological community has lagged behind the biologists in providing information of a popular kind; brochures and posters describing the flora and fauna of the parks seem to be readily available at most park headquarters and in tourist information centres. And park administrators have in the main paid only scant attention to geology in their education programs.

This lack of geological information applies in spite of the fact that our major parks are sited where they are, precisely because of the bedrock geology. This is the feature which controls relief, landforms, and soils, which in turn provide the variety of habitats exploited by a range of plant and animal communities.

It is of interest to note that geology, or geologically related considerations, do figure significantly in the criteria for World Heritage listing. Article 2 of the World Heritage Convention states that properties nominated should (i) 'be outstanding examples representing the major stages of the earth's evolutionary history', and (ii) 'be outstanding examples representing significant ongoing geological processes'. For all the importance accorded geology in the formal definition of these areas, the lack of attention given to it in public education is surprising.

A new project, developed within the Environmental Geoscience Unit in BMR, will go some way towards filling the gap in public awareness of the geology of our major national parks. The initiation of this project just preceded the release by BMR of a comprehensive map of the geology of the Kosciusko National Park. This is the product of earlier mapping carried out by BMR, the Geological Surveys of New South Wales and Victoria, the Australian National University, and Latrobe University.

The map, at a scale of 1:250 000, is a compilation from eight 1:100 000 Sheet areas. In addition to bedrock geology, the park boundaries are clearly shown, and major walking tracks and old mine sites marked. An enlargement of the Mount Kosciusko area itself shows the major features of the late Quaternary glaciation, including possible and probable extent, and the location of glacial lakes, cirques, moraines, and erratics. The map includes a series of coloured photographs of major landscape features, and the geological history is described in a series of diagrams designed to help the lay reader understand the evolution of the map area.

Work is currently underway on the production of a simplified geological map and booklet for Uluru, and on a series of educational materials for Kakadu.

These products focus on the walking trails in the parks, and aim to draw the attention of park visitors to major features of geological interest. It is hoped that they will also find application in aspects of park management. All of these materials are being developed with the co-operation and assistance of the Australian National Parks and Wildlife Service.

These landscapes portrayed in map form are an integral part of Australian culture. The provision of information on their origins and history must serve to enrich the experience of those who visit them.

The Kosciusko map is on sale in the BMR Bookshop for $12.50.

For further information, contact Dr Elizabeth Truswell (Environmental Geoscience Unit) at BMR.

Mapping the offshore Maryborough Basin aboard RV *Rig Seismic*

In December 1989, a team of 21 BMR scientists and technicians successfully completed a four-week geophysical and geological research cruise off southeast Queensland aboard RV *Rig Seismic*. The 'Maryborough' cruise, BMR Survey 91, collected multichannel seismic (MCS) and other data to establish the structural and seismic stratigraphic framework of the offshore Maryborough Basin and investigate its petroleum prospectiveness. As part of this investigation, the wide continental shelf between Fraser Island and Moreton Bay was mapped to delineate a possible extension of the Maryborough Basin, or undiscovered basins, in this area. Additional lines were surveyed at the northern end of the Tasman Basin and across the Capricorn Basin to (i) provide stratigraphic control by seismic ties to the only deep offshore exploration wells in the region, Capricorn 1A and Aquarius 1, and (ii) collect the first high-quality, deep-penetration MCS data in this area for the study of crustal structure, tectonic evolution, and basin development.

The basin and its exploration

The Maryborough Basin, located adjacent to the southern Queensland continental margin (Fig. 5), is a deep trough of Upper Triassic to Lower Cretaceous sedimentary and volcanic rocks. The prospective Lower Cretaceous sedimentary section alone is known to attain a thickness of about 5 km. Deformation in the Late Cretaceous produced a series of broad, open folds with northwest-trending axes north of Maryborough. In the coastal region to the south, deformation was more intense and produced tight to isoclinal folds, faults, and steep dips.

No offshore exploration has taken place since 1970. The offshore part of the basin has not been tested by drilling, and only limited exploration drilling has been done onshore.

Evidence of a possible southeastern extension of the Maryborough Basin comes from recent (1986–87) BMR aeromagnetic surveys, which have provided detailed coverage over much of the Maryborough Basin. These surveys were flown at an altitude of 150 m above ground level, with 1.5-km line spacing, and have contributed an important new data set for interpreting the geological structure of the basin. The new maps clearly define the deep sedimentary trough of the northwest-trending Maryborough Basin. The contours suggest that the Maryborough Basin extends out onto the continental shelf southeast of Fraser Island. However, the limited offshore coverage (10–30 km) of the aeromagnetics does not allow the basin to be traced far onto the shelf.

Marine geophysical surveys of the 1970–73 continental margins program cover the offshore area, and examination of these data reveals at least limited basin development. The sparker seismic records of this old data set are of only poor-to-fair quality, and show little penetration due to the low-energy source.

Petroleum potential

The Maryborough Basin sequence comprises:

- Lower Cretaceous
  - — Burrum Coal Measures 1700–3000 m thick
  - — Maryborough Formation 2150 m av.
  - — Grahams Creek Formation 1200 m approx.
- Lower Jurassic
  - — Tiaro Coal Measures 1350 m min.
- Upper Triassic—Lower Jurassic
  - — Myrtle Creek Sandstone 450 m max.

The Myrtle Creek Sandstone has reservoir potential, while the overlying Tiaro Coal Measures are a possible source formation. However, the largely volcanic Grahams Creek Formation has generally been regarded as economic basement, and the overlying Maryborough Formation is considered to have the greatest petroleum prospects. It not only contains source rocks but some of its sandstone members have reservoir potential; structural closures and minor stratigraphic traps are also present. Gas flowed from the 'lower sandy

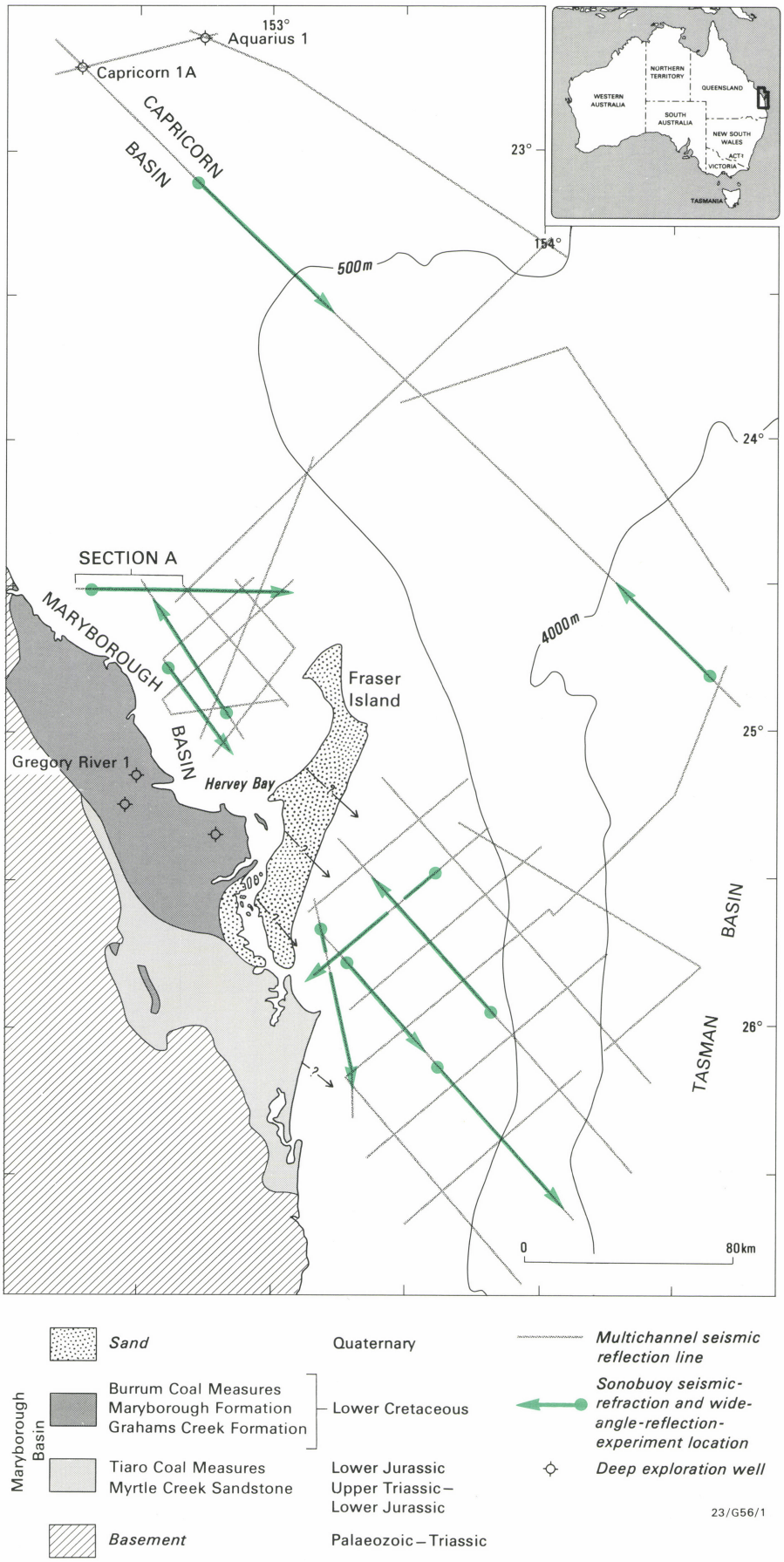

Fig. 5. New geophysical survey coverage by RV *Rig Seismic* over the offshore Maryborough Basin and adjacent areas. The possible southeastern extension of the basin beyond its previous supposed limits is indicated by arrows broken by question marks.

member' of the Maryborough Formation in SDA Gregory River 1 well. Though containing source material, the Burrum Coal Measures appear to lack suitable reservoir rocks.

Data acquired

The *Rig Seismic* cruise resulted in the acquisition of 2900 line-km of high-quality multichannel seismic reflection data (Fig. 5). The 24-fold data were recorded at a ship's speed of 5 knots using a 2400-m 96-channel streamer and dual-tuned airgun-array source (52 L capacity); the record length was 12 seconds, to facilitate definition of deep structure. In addition, a total of 10 sonobuoy refraction and wide-angle-reflection experiments were successfully completed along selected parts of the seismic lines.

Gravity and bathymetric data were collected along all lines in the study area; coverage amounted to about 3600 line-km. The magnetometer was deployed along all parts of seismic lines, except those in shallow water close inshore and within Hervey Bay; it acquired 2450 line-km of magnetic-profile data.

Post-cruise processing of the non-seismic (navigation, bathymetric, and geopotential) data is nearing completion, while processing of the seismic data is well advanced.

Preliminary results

The Hervey Bay seismic monitor records outline a major north-northwest-trending synclinal structure in the Lower Cretaceous formations; visible penetration is limited to about 1.4 s twt in the monitor records. A preliminary stack section (Fig. 6) indicates a large, faulted syncline of Lower Cretaceous sediments blanketed by a flat-lying Tertiary cover several hundred metres thick. The eastern flank of the syncline is cut by an east-dipping fault with large displacement. The Tertiary section is not affected by the faulting. The observed structures may be related to transtensional rifting preceding the opening of the Tasman Sea. The lowest horizon in Figure 6 — probably the volcanic Grahams Creek Formation — lies at a depth of almost 3s twt (about 5.5 km).

Southeast of Fraser Island, the Tertiary cover on the shelf thickens towards the shelf edge, and is underlain by a prominent unconformity. Well stratified prograding sections at the shelf edge are up to 1.5 s twt thick. Structure and stratification beneath the unconformity is difficult to discern on the monitor records because of shallow-water ringing/multiples; however, about 2.0 s twt of section appears to be present on inshore lines near Wide Bay, where a southeastern extension of the Maryborough Basin is expected. Refraction data indicate velocities of 4000–5000 m s^{-2} for the sub-unconformity; velocity surveys in onshore Gregory River 1 well yielded a value of about 4200 m s^{-2} for the Maryborough Formation.

Large areas of the continental shelf are magnetically quiet, implying a thick Mesozoic section or possibly (moderately shallow?) non-magnetic Palaeozoic basement.

The foot of the continental slope is underlain by a thick (ca 3 s twt) pile of post-breakup sediment.

At least 3.0 s twt of sedimentary section is present in deep water at the extreme northern end of the Tasman Basin adjacent to the postulated northeast-trending transform fault which forms the boundary between it and the Capricorn Basin to the north.

Diapiric structures or buried mounds were recorded in the sedimentary section of the southeast Capricorn Basin. They occur in an area where the Capricorn Basin sequence is about 2 s twt thick. The structures have positive seafloor relief of about 200 m, and are 1–2 km in diameter. They probably represent Tertiary volcanic build-ups.

For further information, contact Mr Peter Hill or Mr Chris Pigram (Marine Geoscience & Petroleum Geology Program) at BMR.

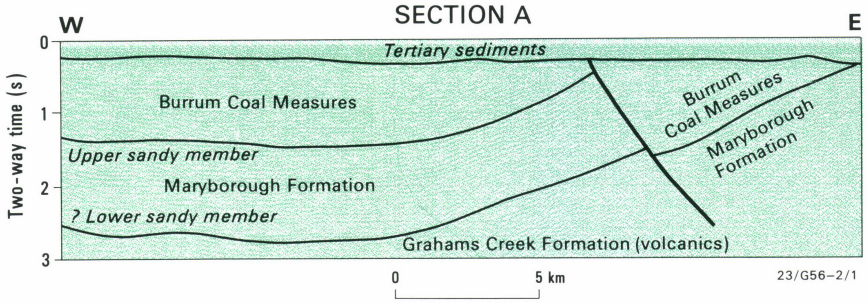

Fig. 6. Preliminary *Rig Seismic* stack section (location shown in Fig. 5) and interpretation across depocentre of offshore Maryborough Basin. The thickness of Lower Cretaceous sedimentary rock (down to the presumed base of the lower sandy member of the Maryborough Formation) is about 5 km. Only the top 3 s of the acquired 12 s data are shown.

Otway Basin petroleum accumulations study completed

A study of the petroleum and other related resources in the Otway Basin was recently completed and has been published as BMR *Australian Petroleum Accumulations Report 6*. The aim of the Otway study, and ongoing studies of other petroliferous sedimenatry basins, is to assist the petroleum exploration industry by providing detailed data sets on the nature, location, and significance of known identified petroleum resources, as well as maintaining an up-to-date strategic inventory of all available petroleum resources.

Petroleum accumulations

A total of 15 petroleum and carbon dioxide accumulations has been identified in the Otway Basin, including the Caroline (carbon dioxide) and North Paaratte (gas/condensate) fields which have been in commercial production for a number of years (Fig. 7).

These accumulations are present in reservoirs contained in the Lower Cretaceous part of the Otway Group, in particular the Eumeralla Formation, and the Upper Cretaceous Sherbrook Group (Waarre Sandstone). The Pretty Hill Sandstone, Eumeralla Formation, and Waarre Sandstone have been the major targets for petroleum exploration wells drilled in the basin.

Reservoir quality

Samples of over 150 core plugs analysed by the BMR Petrophysical Laboratory from over 20 wells drilled in the Otway Basin show that porosities of most of the reservoirs exceed 10%, but — of these — less than one-third have permeabilities exceeding 100 mD.

Reservoir quality and provenance are considered to be some of the most critical elements determining the future petroleum potential of the Otway Basin. Reworked sequences have provided some encouragement because of their enhanced porosity and permeability characteristics.

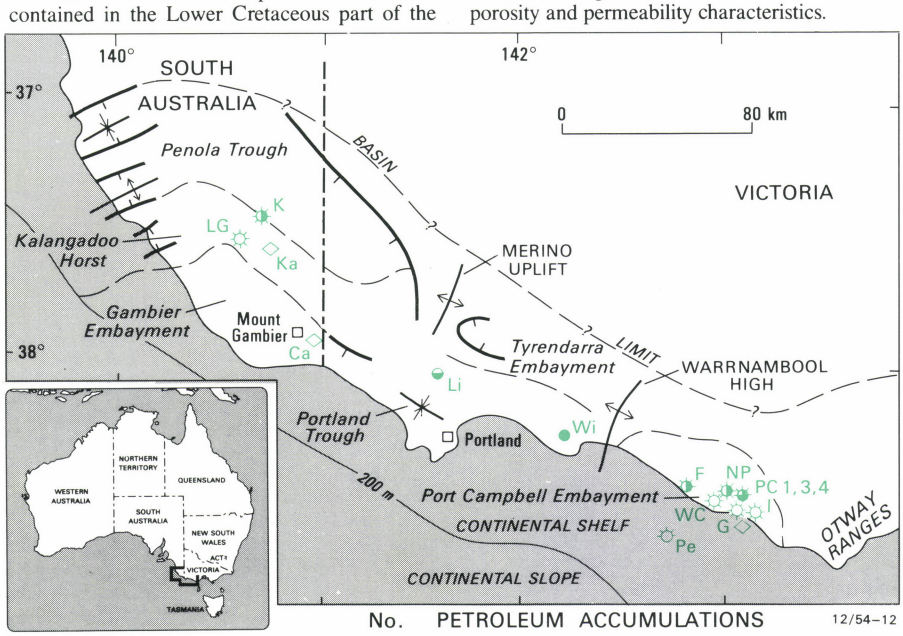

● *Oil*
◒ *Oil show*
☼ *Gas*
☼ *Gas show*
◑ *Condensate*
◇ CO_2

No. PETROLEUM ACCUMULATIONS

Economic and developed

1	North Paaratte	NP	◑
2	Caroline	Ca	◇

Economic and undeveloped

3	Wallaby Creek	WC	☼
4	Katnook	K	◑
5	Ladbroke Grove	LG	☼◇
6	Iona	I	☼
7	Grumby	G	☼◇

Subeconomic and undeveloped

8	Lindon	Li	◒
9	Windermere	Wi	●
10	Kalangadoo	Ka	◇
11	Flaxmans	F	◑
12,13,14	Port Campbell 1,3,4	PC	◑
15	Pecten	Pe	☼

Fig. 7. Petroleum accumulations and simplified onshore structural elements of the Otway Basin.

Source material

The Dilwyn and Paaratte Formations exhibit the highest levels of total organic carbon content, and are potential sources of both oil and gas, although some proneness for gas-generation is evident in non-marine parts of the sequence.

Less than half of all vitrinite readings reported to the BMR Core and Cuttings Laboratory are from shale sequences mature enough to be within the oil window. The results indicate that the oil window is not likely to be encountered at depths of less than 2500 m (Fig. 8).

A notable feature of the Otway Basin has been the detection of at least eight occurrences of coastal bitumen, found to be derived from the atmospheric exposure and biodegradation of mature crude oil. Results indicate that at least some undiscovered accumulations of crude oil occur in offshore subsurface sequences. Periodic strandings of bitumen appear to be derived from these sources.

Petroleum types

The accumulations of natural gas discovered to date range in composition from relatively dry gas (96% methane) to wet gas with notable liquid content, and to accumulations of dry gas mixed with carbon dioxide. Some wet gas accumulations are mixed with carbon dioxide, indicating that the carbon dioxide is not the product of thermal cracking of in-place natural gas. Non-petroleum gases present in some of the Otway accumulations include nitrogen (up to 32.62%) and helium (0.05%), in addition to carbon dioxide.

Production

The Caroline carbon dioxide accumulation has been produced for more than 20 years, supplying much of the demand for this commodity in South Australia and Victoria. Since 1986 the North Paaratte accumulation has been supplying natural gas to domestic and industrial users in Warrnambool. At present the Katnook, Ladbroke Grove, and Wallaby Creek accumulations are the subject of an appraisal study. A decision whether or not to undertake development and production from these accumulations should be made in the near future.

For further information contact Dr Ian Lavering (Production Geology Group) at BMR.

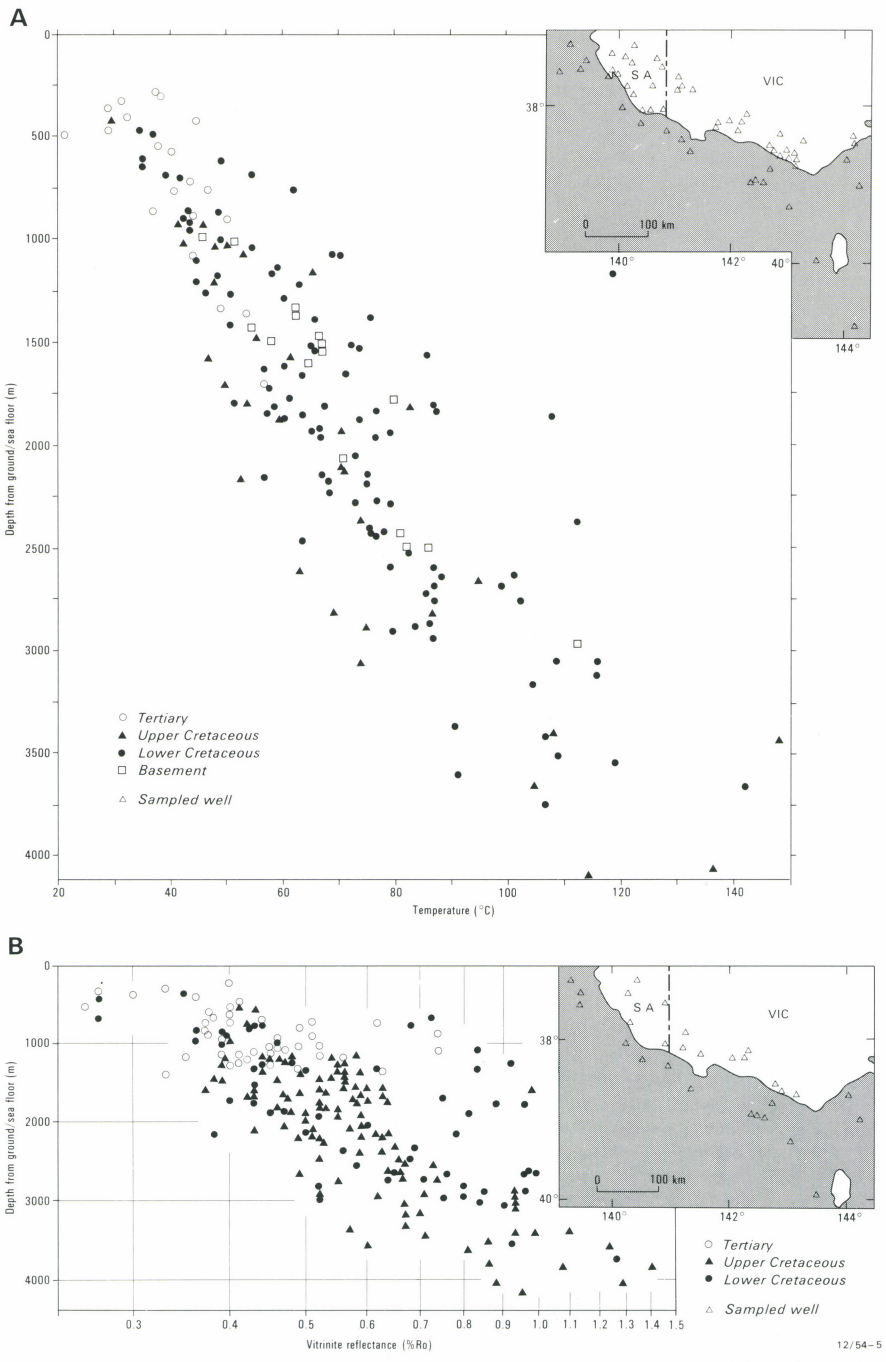

Fig. 8. Plots of temperature and vitrinite reflectance values from samples provided to the BMR Core and Cuttings Laboratory from wells drilled in the Otway Basin.

Distributed image processing at BMR

Last year, BMR installed a state-of-the-art image-processing centre (IPC) based on two SUN Microsystems 4/280 minicomputers, and proprietary hardware and software supplied by International Imaging Systems (I^2S) of California, USA. The IPC provides BMR with the capability to manipulate satellite-derived images, scanned maps, and other Earth-science data sets such as gridded gravity and aeromagnetics. Sophisticated filtering procedures, de-blurring algorithms, and warping and resampling of images to virtually any type of projection can be performed using the I^2S system.

The needs of the many BMR geoscientists who require simple image processing have been catered for by developing an integrated personal-computer-based system. This system uses a commercial PC image-processing package (GEOPAK/RTI) interfaced to the IPC over a high-speed Ethernet local-area network (BMRnet). Images resident on the I^2S system are downloaded to the PC over BMRnet under the control of a PC-resident program. This program, GETIMAGE, which was written in BMR, controls the necessary file transfers and file-format conversions. GETIMAGE firstly uploads a control file to the SUN 4/280, which holds the desired image and then initiates a C shell script. This script converts the image file from its proprietary I^2S format into a line-oriented form which can be used by GEOPAK/RTI. The script also spatially inverts the image in order to accommodate the different origins used by the two systems.

GETIMAGE also controls further processing on the PC of the downloaded image before its use in GEOPAK/RTI. First the data in the file are converted from the IEEE format used by SUN to the inverse IEEE format used by Microsoft in the PC environment. The data are then scaled for use by GEOPAK/RTI and grid and header files are created.

File transfers over BMRnet are accomplished using the TCP/IP services provided by NFS, the SUN Microsystems Network File System. PC-NFS, the PC implementation of NFS, also provides a TELNET capability. Using TELNET, a PC user can remotely log on to the SUN computers in the IPC and run the I^2S display executive or the batch executive. From either of these executives the full power of the I^2S system can be accessed. Sequences of image-processing commands can be executed and the results displayed by using GETIMAGE to download the processed image to the PC.

GEOPAK/RTI has the capability to overlay up to four images. Thus standard remote-sensing techniques, such as the stacking in different colours of separate wavelength bands of the same Landsat scene, can be used. The package can also overlay up to four vector data sets which allows georeferenced data such as geological maps, drainage, and cultural details to be drawn on top of imagery. Labels and line-work can also be applied in a variety of fonts, line weights, and colours. Hard-copy output can be obtained either by using a colour or monochrome printer connected to the PC being used, or by sending the image to the larger-format printer in the IPC.

Any 80286 or 80386 PC fitted with a co-processor and a VGA colour monitor can be used as an image-processing workstation. However, the ideal configuration is an 80386 PC with 4 Mbyte of memory and a minimum of 40 Mbyte of hard-disc storage.

For more information, contact Dr Prame Chopra at BMR.

A new method of dating Australian Precambrian rocks
Accumulated polar wander

Recent studies have enabled BMR palaeomagnetists to distinguish an unexpected characteristic of polar wander that can be applied in a new approach for Precambrian dating by palaeomagnetism. This approach is based on the accumulated angle of polar wander, and is applicable to a wide range of rock types, including sedimentary rocks.

Precambrian dating has used as its time reference principally the half-lives of unstable isotopes in minerals. These techniques have been applied mainly to igneous rocks — preferentially, in the last decade in Australia, to zircon-bearing felsic volcanics and intrusives. Except for occasional dating of diagenetic minerals — especially glauconite — that contain unstable isotopes, the isotopic techniques have not been found suitable for sedimentary rocks.

Non-isotopic dating techniques include palaeomagnetism, where the palaeomagnetic pole obtained from the rock unit of unknown age is compared with dated poles on the apparent polar-wander path. The paths are defined partly by dated poles and partly by poles without dates (Fig. 9). This method has been used many times on the Tertiary weathered profiles in Australia, but it can give at present only very broad age estimates for Precambrian rocks, because the Precambrian paths contain not only large gaps without dated poles but also uncertainties about the location of some of their parts. Moreover, for Australia very few of the dated poles have good age constraints and/or precisely defined coordinates. Because of the complex geometry of the paths, comprising numerous bends, loops, and other irregularities (Fig. 9), it is difficult to estimate ages quantitatively by interpolation, and will continue to be so — even after considerable improvement of the pole paths.

The recent BMR discovery points to a conceptually different way to use polar wander for dating — a way which overcomes the drawbacks with the pole-path interpolation method. Instead of spatial

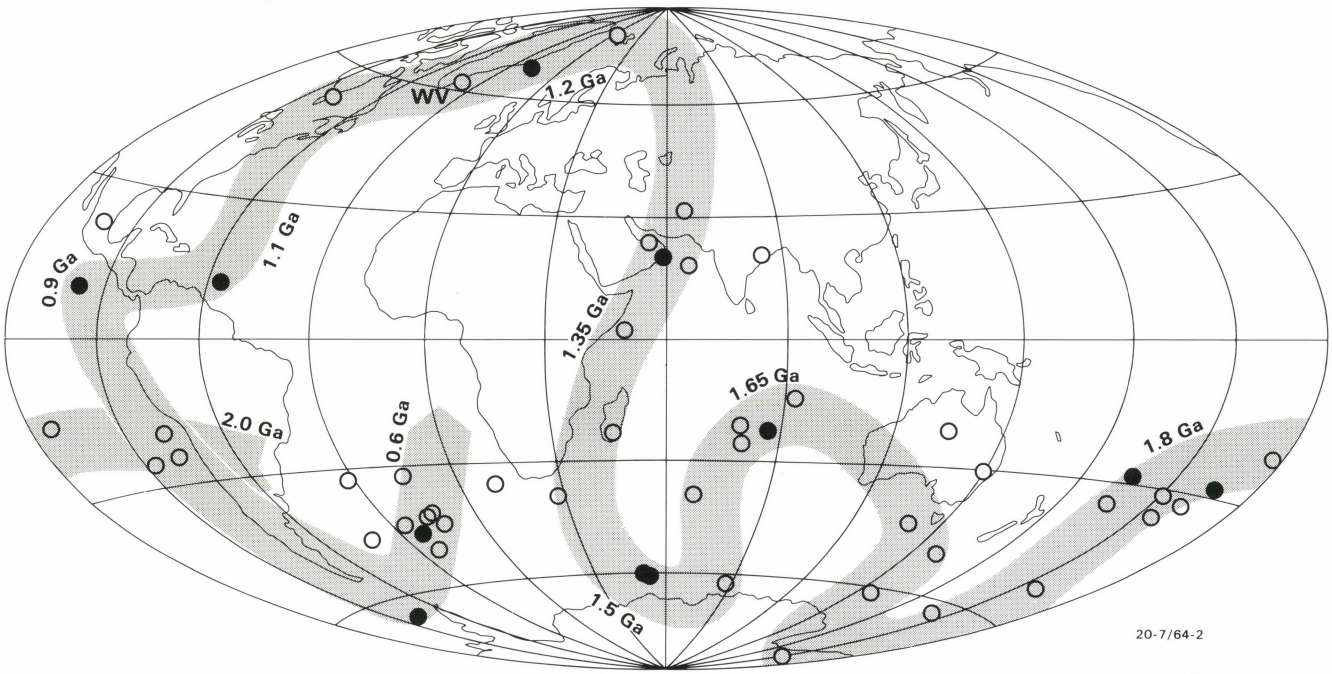

Fig. 9. Apparent polar-wander path for Australia in the period 2.0 to 0.6 Ga (after Idnurm & Giddings, 1988: *Precambrian Research*, 40/41, 61–88). Dated poles are shown by solid circles; undated poles by open circles. The Wooltana Volcanics pole, which is discussed in the text, is labelled WV. The dates indicated along the path are rough estimates based on age-calibrated poles, not on the linear segments.

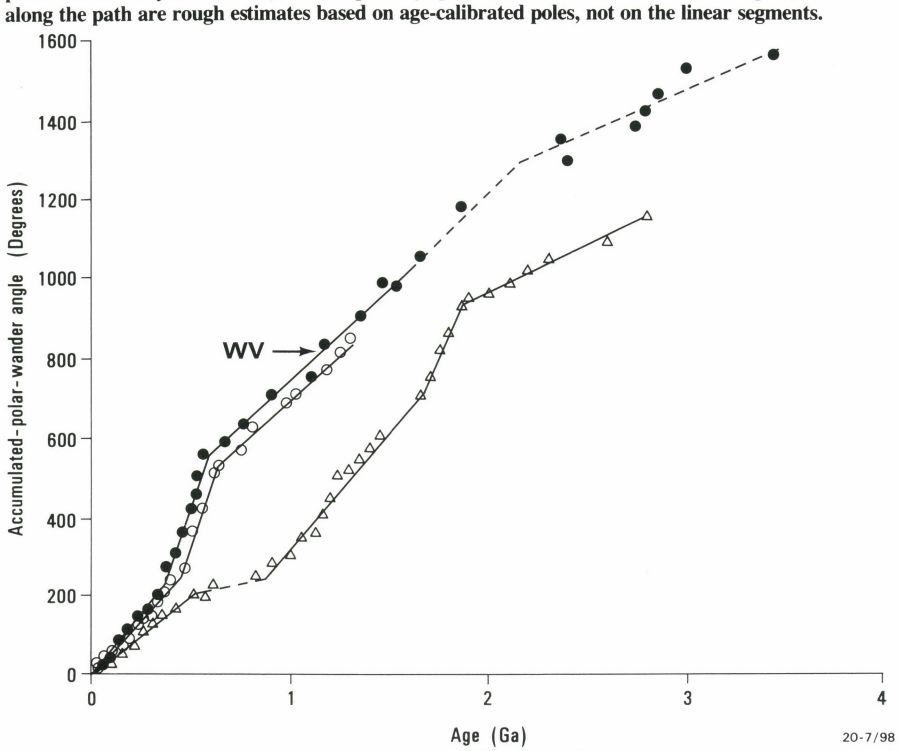

Fig. 10 . Accumulated angle of apparent polar wander through geologic time for Australia (solid circles), Africa (open circles), and North America (open triangles). Linear segments are least-squares regression lines. Poorly defined segments are represented by dashed lines. Arrow indicates the accumulated-polar-wander angle for the Wooltana Volcanics.

presentation of the polar-wander data by points on the globe, the accumulated angle of polar wander is plotted against time (the angle is obtained by dividing the pole path into great circle segments and adding up successively the angular lengths of these segments by scalar addition). A preliminary attempt suggested that such a plot for the Australian Precambrian might consist of straight-line segments (Fig. 10), in contrast to the complex shape of the pole path. This impression was reinforced as additional data were included, and after linear segments were found also in the Phanerozoic plot. To confirm that the linearity is a general feature of polar wander, the plots were then determined for the two other continents that have detailed pole data extending back into the Precambrian — North America and Africa. Those plots were found also to comprise straight-line segments (Fig. 10); moreover, a striking resemblance was noted between the plots for the two Gondwana continents — Australia and Africa.

The linearity in the accumulated polar-wander plots has interesting implications for the Earth sciences: it seems to indicate some unknown mechanism that causes the hidden simplicity in polar wander, and suggests that the geomagnetic field must have been at least approximately dipolar back to the mid-Proterozoic, if not even to earlier times — a fundamental but so far untested assumption of palaeomagnetism which is made, for example, in palaeolatitude determinations. In addition, the plots provide evidence against the

existence of a single long-lived supercontinent (viz., parts of the plot for North America differ from those of Australia and Africa), and suggest major changes in the style of tectonism at geologic times that correspond to the sharp breaks in slope between the linear segments.

The linearity in the accumulated polar-wander plots can be also applied to age dating: the pole for the rock unit of unknown age is plotted on the pole path to obtain its accumulated angle of polar wander; and the age is estimated from that angle using the least-squares regression technique on the corresponding linear segment. (It should be noted that the least-squares regression used assumes that the variances of all the data points are the same; this may not be correct, affecting the statistical rigour.) In this method, the sparseness of pole data does not present as acute a problem as it does with the pole-path method: relatively few well-dated points are required to define a least-squares regression line, but the line's precision is expected to increase with additional data points.

At present the best time interval in the Precambrian for dating Australian rocks by the new technique is 1700 to 550 Ma. Beyond 1700 Ma, the technique should be used with caution because the linear segment is not well defined. The interval 1700 to 550 Ma is constrained by ten dated points, of which one appears to be anomalous. The latter comes from the Eastern Creek Volcanics of the Mount Isa Block, and is currently being redetermined.

What kind of precisions can be achieved with the new method for Australian Precambrian rocks? As an example, consider the Wooltana Volcanics at the base of the Upper Precambrian sequence in the Adelaide Geosyncline. The age of these volcanics has not been settled despite its importance in defining the beginning of the Upper Proterozoic. One possibility, suggested by lithological resemblance, is that the volcanics were extruded at the same time as the 1110 to 1200 Ma Beda Volcanics on the Stuart Shelf, which flanks the geosyncline. According to the palaeomagnetic results of McWilliams & McElhinny (1980: *Journal of Geology.*, 88, 1-26) on the Wooltana Volcanics (pole WV in Fig. 9), and provided that the primary component of remanence has been identified correctly in those results (the volcanics have been altered several times, giving a multicomponent magnetisation), the age of the volcanics is estimated from the accumulated angle (WV in Fig. 10) as 1158 ± 51 Ma (95% confidence limits) if the apparently anomalous Mount Isa pole is included in the regression relation, and as 1148 ± 45 Ma if it is omitted. This estimate is provisional, subject to redetermination of the Mount Isa pole. The precision is governed by both the statistical confidence for the least-squares regression line and the precision of the Wooltana Volcanics pole, which is relatively poor (A_{95} = 17°). The precision would decrease towards the ends of the 1700 to 550 Ma linear segment.

Although additional Precambrian poles in the future may be expected to increase considerably the precisions achievable by the accumulated-polar-wander method of dating, this method is unlikely to yield the typical very high precision obtained by U-Pb zircon dating. Nevertheless, the palaeomagnetic method has the advantage over the latter that it can be used to date a wide variety of rocks such as sedimentary sequences, chemical deposits, basic igneous suites, and possibly some metamorphics (i.e., for dating retrogressive metamorphism). Further, like the Ar^{40}-Ar^{39} method, the new method may be able to date different events in the history of the rock unit — such as reddening, mineralisation, and metasomatism. The linearity phenomenon in accumulated-polar-wander plots therefore appears to provide a useful dating tool for the Precambrian, with good prospects for continued improvement.

For further information, contact Dr Mart Idnurm (Geophysical Observatories & Mapping Program) at BMR.

BMR completes a pilot Geographic Information System

The Kakadu GIS

In co-operation with GEOVISION, BMR has completed a major Geographic Information System (GIS) package on the original 2300 km² Kakadu Conservation Zone, which is now installed at NRIC. This package was a pilot study for BMR with the aim of testing the capacity of GIS in two main ways — firstly as a tool for resolving competing land-use issues, and secondly as a method of storing and manipulating geoscientific data. The Kakadu Conservation Zone project was chosen for the pilot GIS for several reasons, the most important being that nowhere else in Australia was there such a comprehensive number of available data sets covering both geoscience and land-use issues. This article describes the data sets that were entered and some of the problems that were encountered, and evaluates GIS as an aid to geoscientific mapping and land-use issues.

Data entry

Geological maps. The Conservation Zone is covered by some of the most detailed and accurate 1:100 000 geological maps available. These had to be translated into digital format so that they could be interrogated within GIS. A scanned image in raster format direct from the scanner is not suitable because it is not intelligent — i.e., has no attribute data. Digitising the maps by hand proved to be quicker than scanning them and then editing the data manually; the 1:25 000 compilation maps were used for areas with most detail. Part of the problem in the Kakadu area was caused by the extreme detail displayed on the maps; even the colour separates used in the printing of the maps proved to be too detailed. The important point highlighted by this exercise is that traditional geological map production does not produce maps that are easily scannable and capable of being interrogated.

Geophysics. The data set includes magnetic (TMI) and radiometric (potassium, thorium, uranium, and total-count) data collected by BMR in 1988 over 14 819 line-km flown at a nominal spacing of 250 m and nominal terrain clearance of 100 m. The data were entered into an ORACLE table with seven attributes, of which two are the location coordinates and the others are the value for each particular channel (TMI or U or Th, etc.).

Once entered, they could be generated as three-dimensional coloured images by using the digital terrain modelling capacity of GEOVISION. In this format, the data could be interrogated as any other ORACLE data set and colour-coded. More importantly, ratios of the radiometric channels (e.g., U^2/Th) could be calculated and displayed in this format. Once the three-dimensional images were generated, other data sets could be readily superimposed on them — such as the locations of uranium deposits relative to the uranium channel, or the Th values from the whole-rock geochemical database compared with the Th geophysical image.

Mineral deposits. A mineral deposits database using the BMR MINDEP data system was compiled and developed for all publicly available information on 54 deposits, prospects, and occurrences in the original Kakadu Conservation Zone.

Field data. All the field data were collected using traditional pens and field notebooks. With GEOVISION, one capacity of the system allows data from field notebooks and field sketches to be scanned and stored as point-source data. Information from contractors' reports could also be stored. At any one point location, all observations from any geologist could be examined, making comparison of different interpretation of the one outcrop easy!

Vegetation. A digital vegetation map at 1:250 000 scale was purchased from the National Parks and Wildlife Service.

Geochemistry. Two ORACLE geochemical databases were incorporated in the GIS: stream-sediment and whole-rock geochemical data from PETCHEM, the BMR geochemical database.

Remote sensing. Four Landsat TM scenes covering Coronation Hill had first to be stitched together and then entered. The sheer size of this combined image caused restrictions; eventually only one band was entered and could only be used as an overlay.

Sacred sites. Maps were obtained from the Aboriginal Sacred Sites Authority. At their request, these were entered as a confidential layer, visible only to authorised personnel.

Biological surveys. The recently published work of CSIRO on the whole of Stage 3 of the Kakadu National Park was entered in a simple format (Woinarski & others 1989: *CSIRO Division of Wildlife Report).* Each site was recorded as a location in one database, whilst the other database stored species names and the locations at which they occurred. This enabled the location of each of the sites to be plotted, and the sites at which individual species occurred to be displayed.

Mining tenements. These data were obtained from a third party, and showed all current leases and mine-lease applications.

Evaluation

For land-use issues, GIS is invaluable. All competing data sets are placed on the one system, and meaningful comparisons can be made between vastly different data sets, with the computer in effect becoming the independent arbitrator in response to interrogations such as: 'What was the closest location of one of the sightings of endangered species to Coronation Hill?'; 'How many airbone geophysical anomalies coincide with sacred sites?'

The possibilities for geoscientific manipulation are endless. Examples of the types of comparisons that can be made include combining uranium values from the whole-rock geochemical database with the uranium channel of the geophysical survey to approximately calibrate the survey, and also to check which geophysical anomalies correspond to natural high levels of uranium, which are so abundant in the Kakadu region. Another manipulation is to combine the geophysical anomalies with MINDEP to detect which of them are not related to known occurrences of mineralisation.

One of the greatest assets of GIS is the amount of information collected during a field survey that can be stored and eventually become publicly available. GIS is essentially scale-independent. All information is location-coded and can be presented in map form at a wide range of scales. This tends to make it a more factual system than the conventional hard-copy maps and reports, on which limitations of size, production scale, and costs inevitably lead to much useful information being left in field notebooks or on airphoto-overlays. With GIS, regardless of the scale of production of the final map, no information need be lost. Maps may be produced at 1:250 000 scale, but companies will still have ready access to the actual locations of outcrops where, for example, hydrothermal breccias or quartz vein systems were observed, and the authors' observations.

GIS is already leading to a revolution in geological thinking, whereby new advances are made because of the capacity to integrate many varied data sets and compare features that probably were too difficult to compare in the past. It will help specialists to broaden their interests into other fields, as comparison of data sets from similar locations is so easy.

For further information, contact Dr Lesley Wyborn (Minerals & Land Use Program) at BMR.

High platinum potential in the Lachlan Fold Belt

An earlier report (*BMR Research Newsletter*, 8, 13-14) predicted that the Lachlan Fold Belt might have significant precious-metal potential because of the widespread occurrence of unusual mantle-derived magmas of Ordovician age. A model for the genesis of these magmas suggested that they would have been precious-metal rich when they left the mantle. The model also suggested that fractionation would further concentrate these precious metals because the magmas were undersaturated in sulphur. In this follow-up article, new analyses are presented that confirm these predictions. In addition, it is now becoming clear that mobilisation of platinum group elements (PGEs) can occur in a wide variety of environments at temperatures below magmatic conditions. Accordingly, a number of specific areas in the Lachlan Fold Belt can be targeted as prime areas for the concentration of platinum by secondary processes.

The products of Ordovician magmatism are concentrated into four main belts in the Lachlan Fold Belt (Fig. 11). These are, from west to east: (1) Fifield-Nyngan, where the magmatism produced mid-crustal intrusive complexes that are anomalously high in platinum and have been the focus of intensive exploration over the last few years; (2) Parkes-Narromine, where high-level intrusive complexes containing porphyry-style Cu/Au deposits are associated with thick accumulations of volcanics; (3) Orange-Wellington, similar to (2), containing several operating Au mines; the Ordovician volcanics at Kiandra (southern NSW) may be an extension of this belt from beneath younger rocks, as suggested by Owen & Wyborn (1979: BMR *Bulletin* 204); (4) Sofala-Rockley, where altered and deformed volcanics are associated with a few related intrusives.

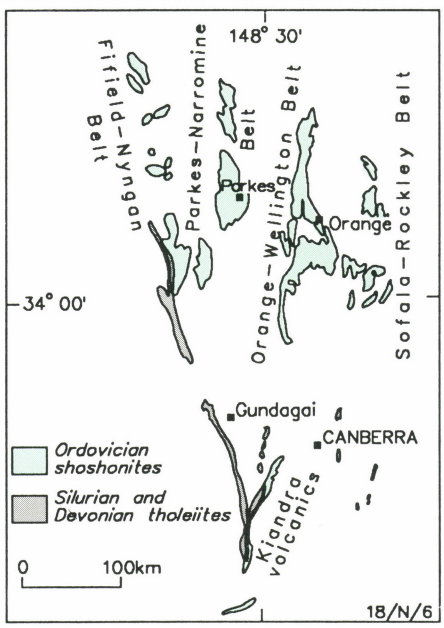

Fig. 11. Mafic rocks, central Lachlan Fold Belt.

The magmatic rocks of all four belts are potassium-rich. They are mainly basalts, though for many years the volcanics were erroneously regarded as mainly andesitic, a conclusion that led to the development of a plethora of island-arc tectonic models. The basalts plot on mantle-normalised chemical variation diagrams (spidergrams) with distinctively high Ba, K, Sr, and P, and low Nb, Zr, and Ti (Fig. 12). These chemical characteristics are indicative of rocks of the shoshonite association.

As part of the National Geoscience Mapping Accord, BMR and the Geological Survey of New South Wales have commenced geological studies in the Orange-Wellington belt. Emphasis has so far been on mapping and sampling the volcanics and associated intrusives. Standard major and trace-element analyses carried out for 60 samples are held in BMR's Petchem database.

Aliquots of 50 g of selected samples were analysed by fire assay, followed by ICPMS for Pt, Pd, and Au. These samples have Pt abundances of typically 5 to 10 ppb, and Pd 10 to 20 ppb, or 10 to 20 times higher than tholeiitic rocks from the Lachlan Fold Belt (Figs. 13 and 14). Gold contents are mostly lower than Pt or Pd (2 to 5 ppb), and are

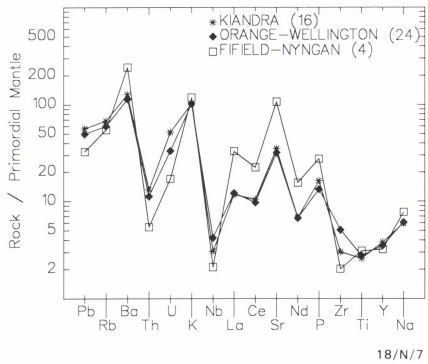

Fig. 12. Average trace-element contents of analysed samples of Ordovician mafic rocks from the Lachlan Fold Belt. Numbers in parentheses refer to numbers of samples averaged.

highest in the least altered and metamorphosed samples. The data indicate that Au has probably been removed from the rocks during burial metamorphism, perhaps into the vein deposits that are known throughout the region. As sulphur contents are low (typically < 200 ppm), magmatic fractionation probably proceeded in a state of sulphur undersaturation, so that precious metals might be expected to have concentrated during fractionation. However, more magnesium-rich intrusive rocks that are dominated by olivine accumulation are high in Pt (ca 20 ppb) and low in Pd (ca 2 ppb), in contrast to the non-cumulate extrusive rocks, and there is a systematic decrease in Pt/(Pt+Pd) with decreasing Mg number (Fig. 15). These data suggest that Pt and Pd were decoupled during fractionation, and that Pt was concentrated by an early-formed cumulate phase.

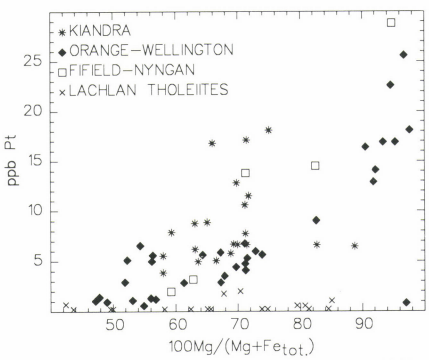

Fig. 13. Plot of Pt *v.* Mg number.

The relatively high Pt-to-Pd ratio in the magnesium-rich rocks is a characteristic of Pt mineralisation associated with Alaskan-type zoned complexes such as those in the Fifield-Nyngan belt, and elsewhere in the world (Urals, USSR, and Tulameen, Canada). This high ratio does not extend through to the non-cumulate volcanic rocks in the Lachlan Fold Belt. Chrome-rich spinel is a common accessory in the olivine cumulates, and could be the cause of the decoupling. Capobianco & Drake (1990: *Geochimica et Cosmochimica Acta*, 54, 869-874) carried out experiments that showed that Pd is incompatible in spinel, and that two other PGEs (Rh and Ru) are highly compatible, but they have no data on Pt. Amossé & others (1990: *Chemical Geology*, 81, 45-53) suggested that, at the high oxygen fugacities found in Alaskan-type complexes, chrome spinel and Pt-Fe alloy (90% Pt) are stabilised, and they crystallised Pt-Fe alloys in their experiments. However, they offer no explanation why Pd is not also taken up by the alloy. At high f(O2) Pt-Fe alloys should be stable over a wide range, so perhaps it is the low sulphur fugacity that allows the precipitation of Pt-Fe alloys. The key, then, to understanding why Alaskan-type complexes and the olivine-rich cumulates from the Lachlan Fold Belt have high Pt/Pd could lie in the understanding of the Fe-Pt-Pd alloy system. Pt-Fe alloys containing 80-90% Pt and only 2-3% Pd are an important component of the Pt mineralisation in the Fifield-Nyngan belt (Johan & others, 1989: *Mineralogy & Petrology*, 40, 289-309).

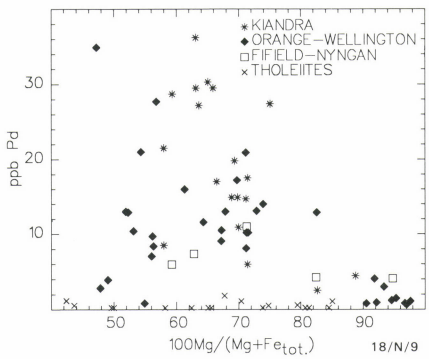

Fig. 14. Plot of Pd *v.* Mg number.

Evidence pertaining to the secondary mobilisation of PGEs in a wide variety of environments has grown in recent years (e.g., Balhaus, 1988: *Economic Geology*, 83, 1140-1158; Boudreau, 1990: *Tenth Australian Geological Convention, Abstracts*, 131-132). The high Pt and Pd contents of Ordovician magmatic rocks in the Lachlan Fold Belt might have favoured their secondary mobilisation to form concentrations of economically viable deposits. In particular, the high content of Pt in magnesium-rich rocks could make exploration in and around highly altered rocks of this composition worthwhile. Magnesium-rich highly altered rocks have been reported from the Sofala Volcanics by Barron (1976: *American Journal of Science*, 276, 604-636). Similar, even more altered and perhaps more promising rocks occur in the Rockley Volcanics, in which talc schists are thought to be derived from olivine-phenocryst-rich lavas (Grey, 1981: unpublished BSc (Hons.) Thesis, *Australian National University);* they probably contained about 20 ppb Pt before alteration (see Fig. 13), but their Pt contents after alteration have not yet been established. Altered ultramafic rocks in the Gundagai area (Gundagai Serpentinite) have equivocal relationships with surrounding rocks. They could be infaulted slivers of Ordovician magmatic rocks. A study of their Pt and Pd contents might help resolve their origin and upgrade their prospectiveness.

For further information, contact Dr Doone Wyborn (Minerals & Land Use Program) at BMR.

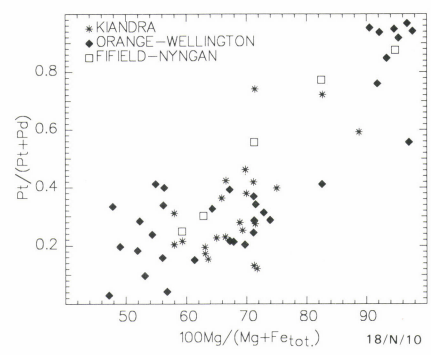

Fig. 15. Plot of Pt/(Pt+Pd) *v.* Mg number.

Geochemical discrimination of mafic layered units, eastern Pine Creek Inlier

New studies of existing geochemical data from layered mafic rocks in the eastern Pine Creek Inlier have discriminated several distinct compositional types among them. Thus, the pre-orogenic Zamu Dolerite of Ferguson & Needham (1978: *Journal of the Geological Society of Australia*, 25, 309-322) comprises three compositional types: the northeast Zamu (NEZ) dolerite northeast of the Jim Jim Fault Zone; the Zamu Dolerite s.s. in the South Alligator Valley; and the Burrundie Zamu (BZ) dolerite in the Burrundie district (Fig. 16). The Shovel Billabong Andesite appears to be geochemically distinct from the Zamu Dolerite s.s., with which it is closely associated in outcrop. Also, metadolerite in southwest MUNDOGIE* and northern RANFORD HILL — identified as the Goodparla dolerite (revision of Goodpalah Diorite of Gray, 1915: *Bulletin of the Northern Territory of Australia*, 14, 20-31) — is distinct from the Oenpelli Dolerite (Stuart-Smith & Ferguson, 1978: *BMR Journal of Australian Geology & Geophysics*, 3, 125-133), to which it has previously been assigned.

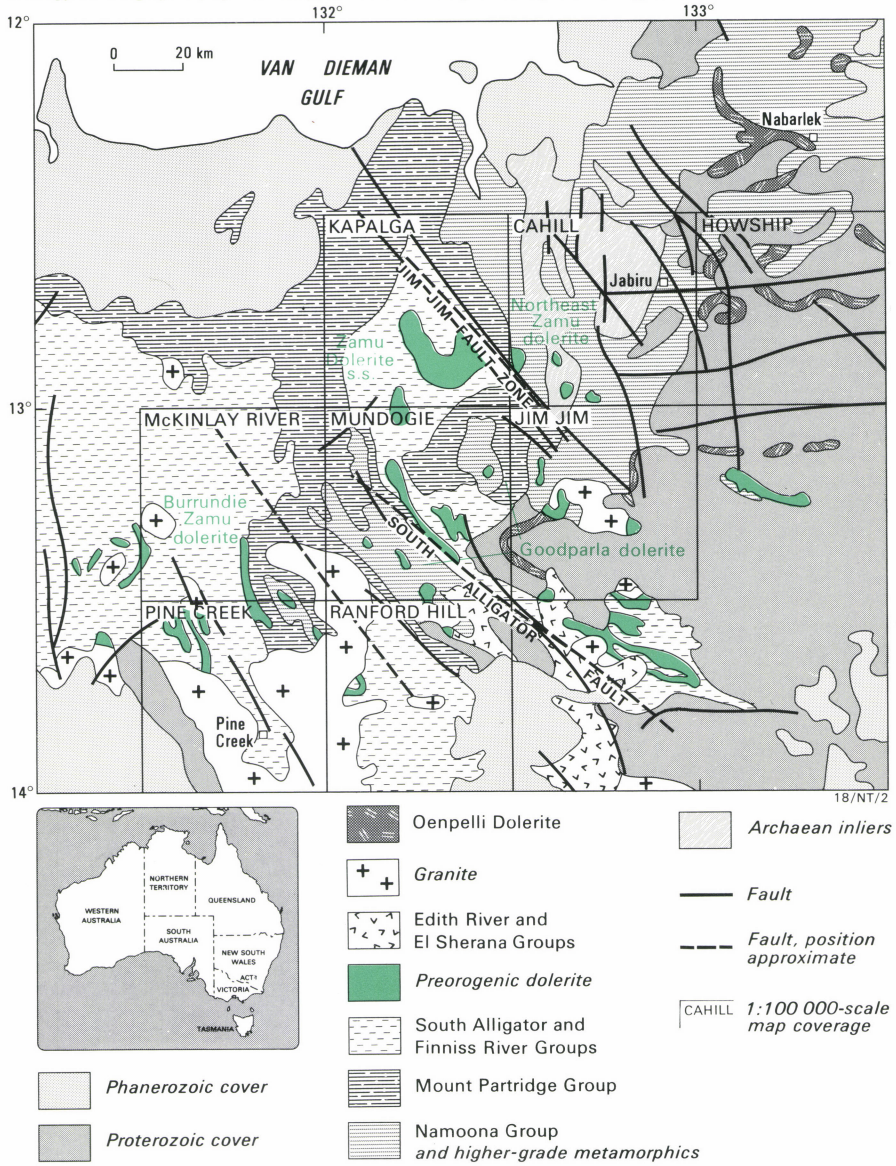

Fig. 16. Distribution of the layered mafic rocks in the Pine Creek Inlier.

Zamu Dolerite s.s.

The Zamu Dolerite s.s. is confined to the area southwest of the Jim Jim Fault Zone, and extends a few kilometres southwest of the South Alligator Fault. It is the most siliceous of the units previously included in the Zamu Dolerite s.l. Although its samples show a tholeiitic iron-enrichment trend, analyses fall mainly within the calc-alkaline field in an AFM plot (Fig. 17). In a plot of normative plagioclase against Al_2O_3, most of its samples lie on the tholeiitic side of the dividing line proposed by Irvine & Baragar (1971: *Canadian Journal of Earth Sciences*, 8, 523-548), but it forms a trend closer to the calc-alkaline field than other units of dolerite. It has a well defined fractionation trend (e.g., Fig. 18) which is quartz-normative throughout.

The corresponding evolution in mineralogy of the Zamu Dolerite s.s. progresses from early cumulus orthopyroxene with clinopyroxene, through augite-pigeonite (now mostly inverted), to upper units with a single pyroxene or brown hornblende. The dolerite is characterised by graphic quartz-feldspar intergrowths, readily recognisable even in specimens from the alteration zones. Available data show platinum group elements (PGE) tend to be concentrated within the fractionation trend, probably with S, and not with early high Cr in the basal zone (Fig. 18).

The Zamu Dolerite s.s. has been sampled only on a regional basis, so its potential as a source for the PGE in the Coronation Hill orebody cannot be appraised. In its weathered outcrops beneath the flood plain of the South Alligator River, it may also have some potential for lateritic concentrations (cf. Bowles, 1986: *Economic Geology*, 81, 1278-1285).

* Names of 1:100 000 Sheet areas are printed in capitals.

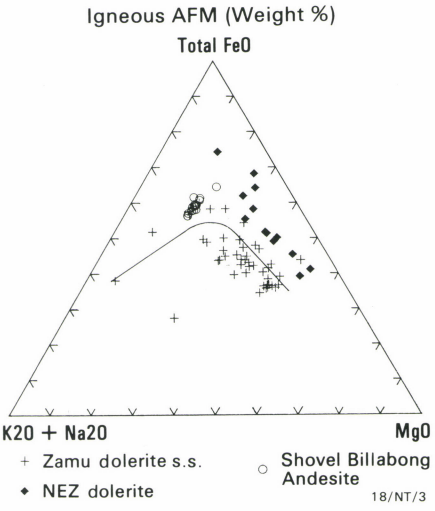

Fig. 17. AFM diagram for the Zamu Dolerite s.s, NEZ dolerite, and Shovel Billabong Andesite.

Shovel Billabong Andesite

The Shovel Billabong Andesite, placed stratigraphically within the South Alligator Group, crops out in the same area as the Zamu Dolerite s.s. Analyses of fine-grained rocks from KAPALGA indicate that it continues farther north than previously known. In the early mapping, it was included with the Zamu Dolerite, but it is now considered to be a single extrusive unit repeated by folding and faulting (e.g., Stuart-Smith & others, 1986: Kapalga — *BMR 1:100 000 Geological Map and Commentary*).

The chemical composition of the Shovel Billabong Andesite places it in the class of basaltic andesites. Most of its samples fall in a tight cluster (Figs. 17 and 18), as befits an extrusive, unfractionated unit. It has a lower mg[+] than most Zamu Dolerite s.s. samples, and carries traces of PGE.

[+] mg = MgO/(MgO + total Fe as FeO).

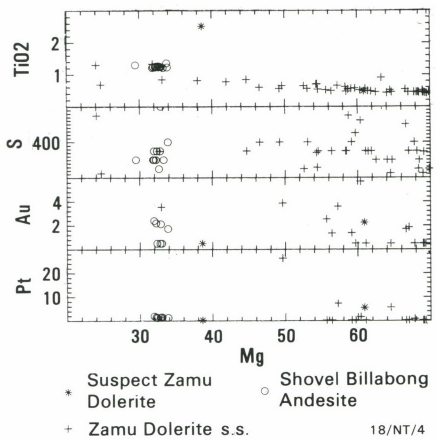

Fig. 18. Au, Pt, S, and TiO_2 in the Zamu Dolerite s.s. and the Shovel Billabong Andesite plotted against mg. Au and Pt in ppb, S in ppm, and TiO_2 in per cent. (Suspect Zamu Dolerite — included in but less siliceous than Zamu Dolerite s.s.)

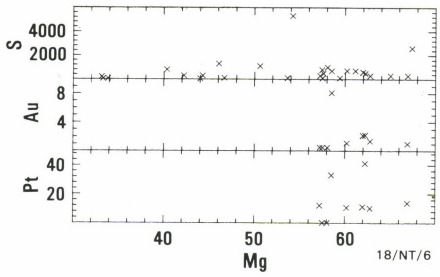

Fig. 19. Au, Pt, and S in the BZ dolerite plotted against mg. Au and Pt in ppb, and S in ppm.

NEZ dolerite

Metamorphosed mafic rocks, mainly amphibolites, have been mapped as Zamu Dolerite s.l. in the northeast Pine Creek Inlier. They include samples from the South Beatrice Window (HOWSHIP), which have high overall Al_2O_3 and compositions so unlike the Zamu Dolerite s.l. that they should be excluded from it. A further set of samples of mafic rocks has geochemical trends distinct from those of the Zamu Dolerite s.s., from which it is distinguished herein as the NEZ dolerite.

Geological maps show the rocks surrounding the NEZ dolerite as units older than the South Alligator Group, principally the Cahill Formation, and metamorphic rocks which may include lateral equivalents of the Finniss River Group, the South Alligator Group and older stratigraphic units.

The NEZ dolerite is quartz normative, like the Zamu Dolerite s.s., from which it is distinguished by its higher colour index, lower differentiation index, less normative plagioclase, and more calcic normative plagioclase at similar mg. Analyses fall on a well defined trend within the tholeiite field on an AFM plot (Fig. 17). The majority of the specimens studied by Ferguson & Needham (1978) were from the NEZ dolerite.

BZ dolerite

The BZ dolerite crops out in the centre of the Pine Creek Inlier as thin sills intruding the Koolpin Formation; in the Burrundie and Golden Dyke domes; north of Ban Ban Springs; and in a belt following the same stratigraphic level north from Francis Creek (McKINLAY RIVER & PINE CREEK). A single sill of dolerite, exposed east of the Cullen Batholith, near McCarthys mine (RANFORD HILL GR845780) is an outlier of the unit. The amphibolites within the Masson Formation east of Francis Creek have compositions which show that they are part of the same unit. Samples from the isolated dolerite within the Burrell Creek Formation (McKINLAY RIVER GR960096) have compositions atypical of the BZ dolerite, and should not be included with it.

Much of the outcrop area of the BZ dolerite lies within the contact zone of the Cullen Batholith. Samples in the collection vary from completely recrystallised to slightly altered. The highest-grade assemblages are in samples from east of Francis Creek, where actinolite is developed and igneous textures completely obliterated. Quartz is less abundant than in the Zamu Dolerite s.s., but graphic intergrowths are present in some samples.

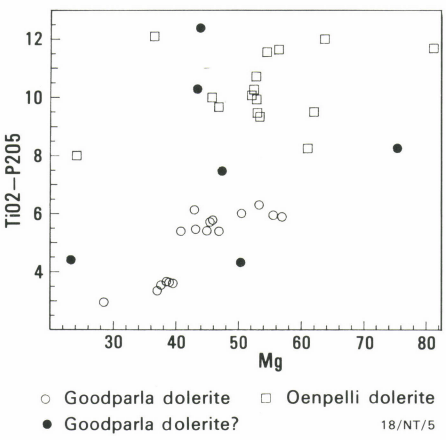

Fig. 20. Plot showing the distinction between the Goodparla dolerite and the Oenpelli Dolerite, using TiO_2/P_2O_5. (Goodparla dolerite? — samples with somewhat similar chemistry from the northeast Pine Creek Inlier.)

The BZ dolerite shows a well defined fractionation trend. It is less siliceous than the Zamu Dolerite s.s., and high mg samples are olivine-normative. Samples from the magnesian end of the trend show significant values of PGE and Au (Fig. 19), but no tendency to form a sharp peak within the series. This may reflect the failure of the thin sills to crystallise in a way that produced an intense concentration of PGE. The results from the samples collected east of Francis Creek have concentrations of Au and PGE similar to those from the sills farther west.

There are no reports of PGE near the BZ dolerite, though the potential for secondary concentrations should be considered. Gold deposits do occur near the BZ dolerite in the Golden Dyke dome and adjacent to the Hayes Creek Shear, but the Koolpin Formation is as likely a source of Au as the BZ dolerite.

Goodparla dolerite

The Goodparla dolerite is a unit of massive dolerite within the outcrop area of the Masson Formation (Nanooma Group) in southwest MUNDOGIE and northern RANFORD HILL. An olivine bearing gabbro intersected in BMR Mundogie 42, in northeast MUNDOGIE, has a composition which lies on the trends for the Goodparla dolerite. The unit has not been traced northeast of this point, though three samples from near Narbalek mine have some chemical affinities with it. Samples of metadolerite from JIM JIM are distinct from the Goodparla dolerite.

All samples of Goodparla dolerite show some effects of metamorphism. Many samples contain olivine or mineral aggregates pseudomorphing olivine. Quartz occurs in some samples and apatite in some. Part of the outcrop immediately to the north of Buk Buk Lookout (MUNDOGIE GR026074) contains large euhedra of plagioclase.

Analyses of the dolerite fall on a well defined trend from olivine-normative at high mg to quartz-normative at low mg. On many plots the samples lie on the same trends as the suite of Oenpelli Dolerite, with which they have been equated. From the present data set, the best discriminants are P_2O_5, TiO_2, and Ba: XY and ternary plots using these elements can be used to separate the two units (e.g., Fig. 20). Analyses of selected Goodparla dolerite samples revealed no significant PGE or Au values. This should not be taken as definitive evidence that the unit is barren, as there is no certainty either that the basal part of the unit has been sampled or that the sampling has been adequate within the unit.

For further information, contact Dr Gladys Warren (Minerals & Land Use Program) at BMR.

ORGCHEM

Organic geochemical database

In response to numerous enquiries by petroleum exploration personnel on the availability of geochemical information, a new database — ORGCHEM — has been created.

This new database is based on the relational database management system ORACLE. ORGCHEM integrates non-BMR and BMR-generated geochemical data. Within ORGCHEM the locality data includes basin, well, formation, and depth, while the geochemical information covers Rock Eval, organic carbon content, and vitrinite reflectance results. This is basic data relevant to organic maturation levels, source richness, and source type, and is of primary importance to petroleum exploration personnel involved in assessing the petroleum prospectiveness of an area or in modelling petroleum generation.

The bulk of the non-BMR-generated information is derived from well-completion reports acquired by BMR through past and present Government Regulatory Acts, PSSA and PSLA (pre-1980 offshore wells only). From these sources, over 12 000 records have been compiled. The Organic Geochemistry Facility within the Onshore Sedimentary & Petroleum Geology Program has undertaken the task of extracting the remaining geochemical data from post-1980 PSLA-acquired well-completion reports.

ORGCHEM also contains all organic geochemical and isotopic information produced within BMR since 1982. The principle source of this information is from organic geochemical investigations undertaken within the Organic Geochemical Facility. Already ORGCHEM contains over 4000 records of 'in-house' generated data.

Concurrently with this data accumulation phase, links with PEDIN (Petroleum Data Exploration Index) are being developed to enable interested persons to perform user-pay customised retrieval of open-file geochemical data for specific, basinal, or regional studies.

For further information, contact Dr Chris Boreham (Onshore Sedimentary & Petroleum Geology Program) at BMR.

New publications on the Amadeus Basin available soon

In 1983, BMR established a project to examine selected aspects of the geology and geophysics of the basin, concentrating in particular on the lower Palaeozoic reservoir and source-rock facies in the northern part of the basin. The publication phase of the project is now close to realisation.

BMR Bulletin 236, 'Geological and geophysical studies in the Amadeus Basin, central Australia' (edited by Russell J. Korsch & John M. Kennard) is a compendium of the geoscientific results presented in 36 papers contributed by 59 authors from BMR, the Northern Territory Geological Survey, industry, and academic institutions. The papers are grouped into the following topics: geological and geophysical setting, Proterozoic stratigraphy and sedimentology, Palaeozoic stratigraphy and sedimentology, palaeomagnetism, structural and tectonic development, deep seismic and teleseismic interpretations, petroleum geology, hydrogeology, and stress regime. It is expected to be available for sale during the first half of 1991.

BMR Bulletin 237, 'Stratigraphy and palaeontology of the Pacoota Sandstone, Amadeus Basin, Northern Territory' (compiled by John H. Shergold) presents the results of combined investigations by BMR, the Northern Territory Geological Survey, and Pancontinental Oil Company Pty Ltd between 1983 and 1988. The Pacoota Sandstone contains important commercial hydrocarbon resources: gas and condensate are produced at the Palm Valley Field, and oil and gas at the Mereenie Field. A detailed analysis of the trilobite biostratigraphy of the Pacoota Sandstone has evinced four stratigraphic sequences, which can be correlated from surface outcrop to well sections that lack biostratigraphic control but are geophysically defined. A basic data bank containing locality, lithological, and palaeontological information is appended. It is expected to be available for sale early in 1991.

Amadeus Basin 1:1 000 000 map folio (compiled by John F. Lindsay) will comprise more than 30 individually authored maps showing water resources, solid geology, structure, cross-sections, stratigraphic chart, seismic shot-points, interpreted seismic sections, and structure contours, isopachs, outcrop distribution, and facies of selected depositional units. It is expected to be ready for printing in mid-1991.

ODP Leg 121 palaeomagnetism gives new insights into the evolution of Broken Ridge, Ninetyeast Ridge, and the Himalayan collision model

Since Australia, jointly with Canada, became a member of the Ocean Drilling Program in 1988, BMR scientists have made considerable contributions to studies arising from several ODP legs. Among them is ODP Leg 121, to which palaeomagnetism has contributed significantly to the main aims: to determine the breakup mechanism of the Kerguelen–Broken Ridge Plateau, the origin of Ninetyeast Ridge, and the evolution of the India–Asia collision.

Points addressed specifically in the palaeomagnetic program were:

- the contribution of thermal expansion above a heat source, and far-field stresses, to the Kerguelen–Broken Ridge Plateau breakup;
- the origin of Ninetyeast Ridge in relation to the Kerguelen hotspot, the Amsterdam–St Paul hotspot, and the Southeast Indian Ocean Ridge; and
- the timing of collision-related slowdown of the Indian plate in the contentious 40–55-Ma interval, and further inferences on the Himalayan continent–continent-collision model.

Kerguelen–Broken Ridge Plateau breakup

The first part of the palaeomagnetic program was dedicated to a detailed magnetostratigraphic study of the pre- and post-rift sedimentary sequence on Broken Ridge (Sites 752–755; Peirce & others, 1989: *Proceedings of the ODP Initial Reports*, 121; Gee & others, in preparation a: *Proceedings of the ODP Scientific Results* 121). This magnetostratigraphic profile helped to date the onset of rifting of the Kerguelen–Broken Ridge Plateau at 45 to 42 Ma. The palaeomagnetic results showed no evidence of pronounced thermally induced magnetic (rifting) overprints. Together with uplift and heat-flow data, this implies that far-field stresses, rather than thermal effects, caused the rifting of the Kerguelen–Broken Ridge Plateau and the attendant uplift of Broken Ridge. Absence of such a rifting overprint markedly distinguishes the Kerguelen–Broken Ridge rifting process from the Late Cretaceous extensional tectonism of the Tasman Sea. Palaeomagnetic and fission-track data from the Tasman seaboard of southeastern Australia suggest that a short-lived thermal pulse around 90 Ma preceded rifting by 5 to 10 Ma.

Ninetyeast Ridge origin

The second part of the palaeomagnetic program was dedicated to a detailed study (Klootwijk & others, in preparation: *Proceedings of the ODP Scientific Results, 121;* Smith & others, in preparation: *ibid.;* & Gee & others, in preparation b: *ibid.*) of 1500 Tertiary and Upper Cretaceous sediment and basement samples from three sites on the southern (Site 756, basement, 43.3 Ma), central (Site 757, 58.5 Ma), and northern (Site 758, 81.9 Ma) parts of Ninetyeast Ridge.

Palaeomagnetic data from the ash and basement sequences of the three Ninetyeast sites and from the pre-rift sequence at Broken Ridge have had considerable bearing on an appraisal of the evolution of Ninetyeast Ridge. The remanence of the basal ash sequence of Site 757, the lower ash and upper flow sequence of Site 758, and part of the pre-rift sequence of Broken Ridge indicate palaeolatitudes at about 50°S, the present latitude of the Kerguelen hotspot, and thus support a Kerguelen hotspot origin for Ninetyeast Ridge. Reversed polarity overprints in the basalt sequence of Site 758 — with a palaeolatitude of about 40°S, the present latitude of the Amsterdam–St Paul hotspot — probably originated during the site's subsequent passage in the vicinity of that hotspot. Aberrant low inclinations, followed downwards by aberrant high inclinations, in the basalt sequence of Site 757 probably reflect basement disturbances associated with a ridge jump from a location close to Site 757 southward over about 11° towards the present Southeast Indian Ocean Ridge. The overlying ash sequence is not affected by this tectonism, which can be dated around 58 Ma; this accords with the age estimate for this ridge jump reached from interpretation of the magnetic anomaly pattern (Royer & Sandwell, 1989: *Journal of Geophysical Research*, 94, 13755–13782).

Refinements to the Himalayan collision model

The Ninetyeast Ridge palaeomagnetic study proved very rewarding in detailing the evolution of the India–Asia convergence, generally taken as the prime example of continent–continent collision. The palaeolatitude results from the basement and Palaeogene sedimentary sequence of the three

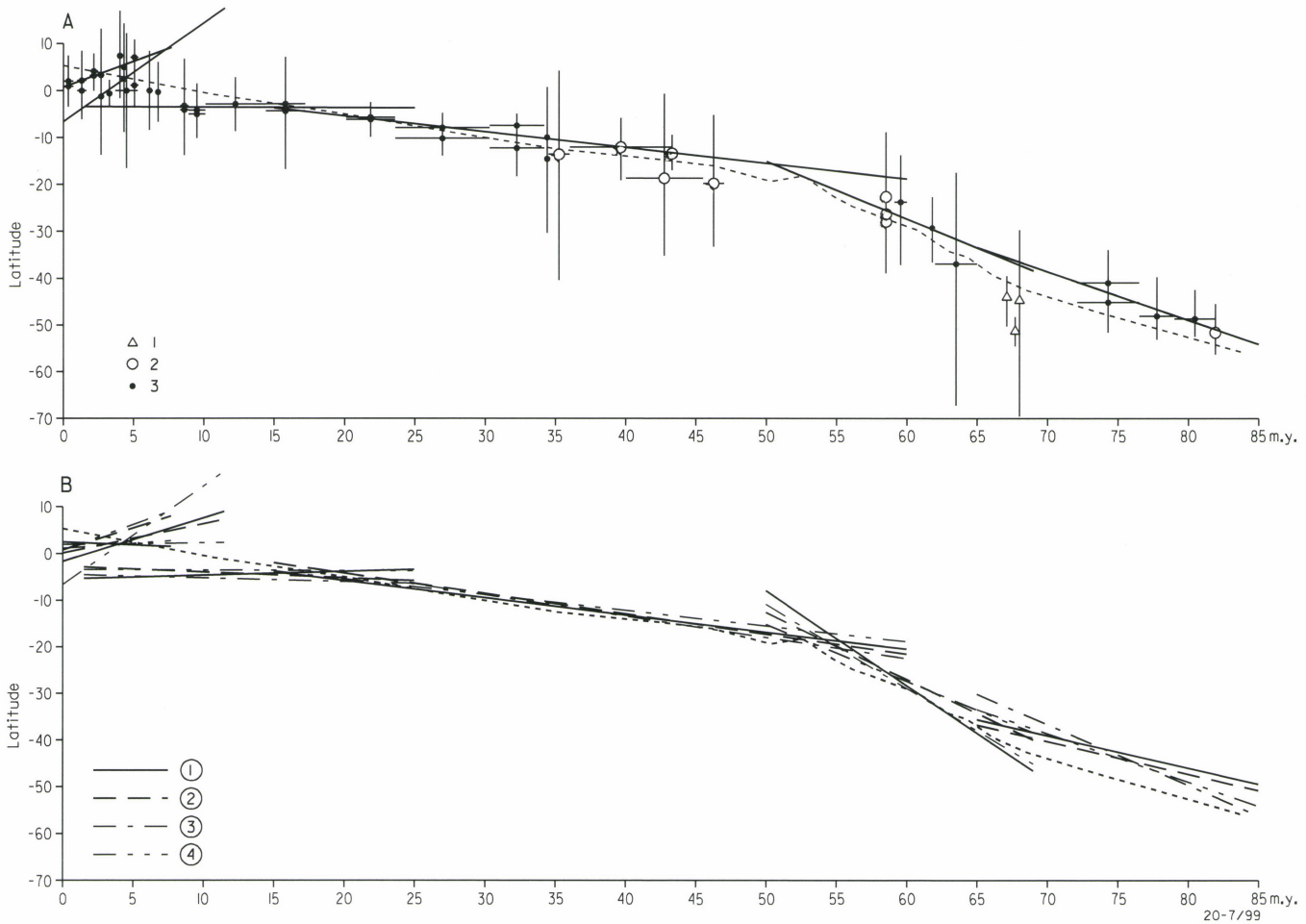

Fig. 21. Weighted linear regression lines fitted to the mean palaeolatitude data from Sites 756, 757 and 758, transferred to Site 758. The horizontal bars indicate the age interval over which individual results have been meaned, and the vertical bars indicate the latitude uncertainty of the meaned result. Figure A shows only results obtained from linear Principal Component Analysis for the harder magnetisation component: 1, 2, mean inclination data obtained from alternating-field (1) and thermal (2) demagnetisation; 3, mean inclination results from the Deccan Traps (India) transferred to Site 758. Figure B combines regression lines fitted to mean palaeolatitudes obtained from both linear (1, 3 [see Figure A]) and planar (2, 4) analysis of the softer and the harder magnetisation components respectively. The regression lines have been fitted over the intervals 0–2.7; 2.7–6.5; 6.5–20.0; 20.0–55.0; 55.0–64.0; 70.0–82.0 Ma; the fitted lines have been extended over 5 Ma at both ends to clarify the intersections.

sites have detailed the Palaeogene collision phase, and the palaeomagnetic signature of the Neogene sequence of the northernmost site (758) has detailed the younger uplift phase of the wider Himalayan and southern Tibetan region.

The India–Asia indentation model developed since the mid-1970s by, for example, Molnar & Tapponnier (1975: *Science,* 189, 419–426) has become a fundamental concept in continental collision tectonics. This model is now applied not only to the evolution of Alpine foldbelts from the Alps in the west to the active northern margin of the Australian plate in the east but also to late Palaeozoic foldbelts, such as the Alleghenian–Appalachian and Hercynian–Variscan systems. Nevertheless, some fundamental questions of southern Asia's tectonics, and the evolution of the Tibetan Plateau in particular, remain hotly debated. Foremost among these is the significance of lithospheric thickening resulting from shortening *versus* large-scale continental subduction. In order to establish this significance, detailed palinspastic control on central Asia's southern and greater India's northern margin, and dating of the uplift of the Himalayan and Tibetan region, are essential.

Unravelling of the Indian Ocean magnetic anomaly pattern by marine palaeomagnetists such as Phillipe Patriat, Jean-Yves Royer, and BMR's David Johnson has delineated in great detail the northwards movement of the Indian plate since its Early Cretaceous breakup from eastern Gondwana. Detailed palaeomagnetic data, however, are needed for absolute positioning through time of Indian and Asian tectonic fragments, and to resolve essential issues such as the timing and palaeolatitude of initial India–Asia contact, the evolution of eastwards-propagating suturing, and the magnitude of India's subsequent indentation into southern Asia. Substantial palaeomagnetic work has been carried out on the Indian continent, the wider Himalayan region, and southern Tibet. However, the palaeomagnetic signature of the heavily tectonised convergence zone shows multiple overprint magnetisations and is difficult to interpret.

Detailed palaeomagnetic studies of undisturbed sedimentary and basement sequences of the oceanic part of the Indian plate are, therefore, of prime importance in establishing the detailed palaeomagnetic control on India's northward movement. Previous palaeomagnetic studies on DSDP cores from Ninetyeast Ridge (Peirce, 1978: *Geophysical Journal of the Royal Astronomical Society,* 52, 277–311) had suggested a slowdown in the northward movement of the Indian plate at 40 Ma, interpreted to reflect collision. An earlier slowdown is suggested, however, from analysis of India–Africa relative-motion data anchored to a hotspot reference frame (50 Ma), and from the geological record of the Himalayan region (53–55 Ma; Patriat & Achache, 1984: *Nature,* 311, 615–621). Klootwijk & others (1985: *Earth and Planetary Science Letters,* 75, 167–183), however, have pointed out that these data and the Himalayan palaeomagnetic record can be interpreted in terms of completion of suturing of greater India and southern Asia at about 55 Ma, with earlier initial contact in northwestern greater India.

The palaeomagnetic data from the ODP sites on Ninetyeast Ridge gave detailed age control on the convergence process. The results showed a complex magnetisation pattern with primary and multiple overprint magnetisations. Mean palaeolatitudes calculated from the primary magnetisation components, transferred to Site 758 and plotted against time (see Fig. 21A as an example), have been analysed for breakpoints following a maximum likelihood and weighted linear regression procedure devised by BMR's Phil McFadden. Most of the so-determined breakpoints (Fig. 21B), however, do not represent changes in India's movement rate. They are interpreted either to reflect lithology-dependent variations in the rock's capacity to retain a primary magnetisation direction (2.7, 6.7, and 18.5 Ma), or to reflect tectonic and/or geomagnetic anomaly problems (63.5 to 67 and 68 to 74.5 Ma). Only the breakpoint at 55+ Ma (minimal age) reliably represents a reduction in India's apparent northward movement rate, from 18–19.5 cm/y to 4.5 cm/y at the location of Site 758.

The 55+ Ma breakpoint is interpreted as completion of the eastwards-propagating India–Asia suturing process. Comparison of the Ninetyeast Ridge data and palaeomagnetic overprints from the Himalaya and Hindu Kush, both to the north and to the south of the Indus–Tsangpo suture zone (Klootwijk & others, in preparation: *op. cit.*), indicates that initial contact of greater India and Asia may have been established already by K/T boundary times. This supports the longstanding notion of Indian geologists that extrusion of the Deccan Traps at K/T boundary time (Chron 29R) was linked to the ensuing deformation of the Indian plate along pre-existing zones of weakness such as the Narmada–Son lineament, and opens new avenues for speculation on a causal relationship between the Deccan Traps volcanism and the K/T boundary diastrophism.

The northernmost site (758; 5°N), on the periphery of the Bengal–Nicobar Fan, gave an unexpected bonus in constraining the Neogene evolution of the convergence zone, with detail probably not obtainable from landbased data. Its Neogene clay-rich sequence shows significant changes in susceptibility and remanence intensity, and is dated through a magnificent magnetostratigraphic profile spanning the last 7 Ma. These changes reflect (with a time lag of up to 1 Ma) uplift and erosional phases in the evolution of the wider Himalayan and southern Tibetan region, as follows:

- 17.5 Ma — initial uplift of the higher Himalaya following initiation of intercontinental underthrusting along the Main Central Thrust; start of Lower Siwaliks sedimentation;
- 10–10.4 Ma — increased uplift, and initiation of the Middle Siwaliks sedimentation;
- 8.9 Ma — probably a tectonic phase whose land-based record is less well confined between 8 and 9 Ma;
- 6.5 Ma — a major tectonic phase evident throughout the northern Indian Ocean and the wider Himalyan region;
- 5.1–5.4 Ma — onset of oroclinal bending in the Himalayan Arc, of extensional tectonism in southern Tibet, and of Upper Siwaliks sedimentation;
- 2.5–2.7 and 1.9 Ma — major phases of uplift of the Himalayan and Tibetan region, culminating in the present-day high relief.

For further information, contact Dr Chris Klootwijk (Geophysical Observatories & Mapping Program) at BMR.

Publications and data released during the period 1 March 1990 - 1 September 1990

BMR Reports

295 Late Cretaceous nannofossil biostratigraphy and biogeography of the Australian western margin

296 Classification and review of the trilobite order Agnostida Salter, 1864: an Australian perspective

BMR Journal of Australian Geology & Geophysics **Vol.11, No. 2 & 3** (Murray Basin Special Issue)

BMR Research Newsletter: **No. 12 April 1990**

The Petroleum Newsletter, **102**

Continental Margins Program Folio **5,** Basins of the Great Australian Bight

BMR Yearbook, **BMR 89**

Geoscience for Australia's future (brochure)

Geoscience maps

1:100 000 geological: **Yeuralba Region,** Northern Territory

1:250 000 geological: **Kosciusko National Park,** New South Wales

1:250 000 geological: **Enarotali,** Irian Jaya

1:250 000 geological: **Fak Fak,** Irian Jaya

1:250 000 geological map and explanatory notes — **Omba,** Irian Jaya

1:250 000 geological: **Ransiki,** Irian Jaya

1:250 000 geological: **Markham,** PNG (reprint)

BMR Records

1989/38 (Australian Phanerozoic Timescales 8) — Jurassic

1989/39 (Australian Phanerozoic Timescales 9) — Cretaceous

1989/41 (Palaeogeography 1) — The Silurian palaeogeography of Australia

1989/49 (Palaeogeography 2) — Notes to accompany a 1:5M scale Devonian structure map of Australia

1990/1 (Groundwater 18) — Sedimentology and diagenesis of the Renmark Group aquifer in Hatfield 1, Murray Basin

1990/2 (Groundwater 19) — Facies analysis of the Renmark Group sediments intersected in Woodlands 1, Murray Basin

1990/5 Aspects of structural geology of the Giles layered basic/ultrabasic complex and associated felsic granulites, Tomkinson Range, Musgrave Block, central Australia

1990/7 The northeast Australian Margin and adjacent areas — a biostratigraphic review and geohistory analysis (Data Package)

1990/8 New data on Mesozoic sedimentary sequences in the Clarence–Moreton Basin, from BMR Warwick 6 and 7 stratigraphic drill holes, New South Wales

1990/11 (Palaeogeography 3) — Australian sea level curves Part 1: Australian inundation curves

1990/15 Index of BMR seismic surveys 1949–1989 (revised edition)

1990/17 Distribution of Triassic reefs in the northern Exmouth Plateau and offshore Canning Basin

1990/18 A field and laboratory study of acoustic impedances of rocks from Tumut, NSW

1990/19 User's guide to the PetChem DataBase

1990/21 (Palaeogeography 6) — Cretaceous source rocks of Australia; interpreted geochemical data

1990/22 (Fossil Fuels 3) — Clarence–Moreton Basin Workshop June 1990. Abstracts

1990/32 Petroleum exploration and development in Australia: a BMR discussion paper

1990/33 Latitudes and longitudes of shots and stations, water occurrences and drilling conditions: Canning Basin seismic survey, 1988

1990/36 Hypocentre relocations using data from temporary seismograph stations at Burakin and Wyalkatchem, Western Australia

1990/37 BMR Marine Survey 46 Lord Howe Rise. Explanatory notes to accompany release of non-seismic data

1990/38 Chemical modelling of lead–zinc transport and deposition in Mississippi Valley-type deposits of the Lennard Shelf, Canning Basin, Western Australia

1990/43 Stratigraphy of Australia's NW Continental Margin (Project 121–26). Research Cruise Proposal (Survey 96)

Bowen Basin tectonic models tested by BMR deep seismic profiles

Within the National Geoscience Mapping Accord, BMR and the Geological Surveys of Queensland and New South Wales have implemented a project to study the structural, tectonic, and thermal histories of the Bowen, Gunnedah, and Surat Basins. Identified as the 'Sedimentary basins of eastern Australia' project, it is planned to run until December 1994. Interpretation of seismic data acquired so far favours both transtension and extension contributing to the generation of the Bowen Basin.

Work commenced with the acquisition by BMR of deep seismic reflection data in the vicinity of Blackwater in the Bowen Basin in late 1989; routine processing of these data is now complete and preliminary results are presented below. Planning is well advanced for the acquisition of deep seismic reflection and refraction data in the Gunnedah Basin in early 1991.

Although the stratigraphy of the Early Permian to Middle Triassic Bowen Basin is reasonably well known, there is some conflict in the models for its development. It has been interpreted as a foreland basin, an extensional basin, and a transtensional (strike-slip) basin. Recently, a mixed-mode origin of extension (or transtension) followed by compression (or transpression) has been proposed. To test various tectonic and structural models, reflection data (20 s two-way time (twt); 8-fold common mid-point (CMP); explosive source) were recorded along three lines totalling 254 km in length (Fig. 22).

Seismic line BMR89.B01 (Fig. 23) was positioned to follow a corridor between two transfer faults postulated by Hammond (1987: *BMR Record* **1987/51,** 131–139), to test the extensional tectonics model. In the west, the Lower Triassic sedimentary rocks are essentially non-reflective, but excellent reflections were recorded from the Upper Permian coal measures below the Triassic rocks. The data suggest that the Permo-Triassic sedimentary wedge thickens to the east, a result which is similar to that seen in line BMR84.14 over the Taroom Trough farther to the south (Korsch & others, 1988: *in* Kleeman, J.D. (Editor) — 'New England Orogen — tectonics and metallogenesis', *University of New England, Armidale,* 134–140). This contrasts with westward thickening predicted by the model of Hammond (1987: *op. cit.*).

The seismic line is dominated by (mid-Triassic?) deformation in the sedimentary succession controlled by thin-skinned thrusting on a series of listric faults which dip to the east and root in a major detachment that also dips to the east (Fig. 23). The detachment appears to flatten in the ductile zone in the middle crust (about 7 s twt). Nevertheless, the Blackwater, Yarrabee, and Dawson structural zones recognised by Hobbs (1985: *Geological Society of Australia, Abstracts,* **17,** 151) exhibit distinct structural styles.

The Blackwater Zone is dominated by reflections dipping gently to the east, interpreted as mainly sedimentary layering (Fig. 23). The Yarrabee Zone is characterised by dome-and-basin structures (Hobbs, 1985: *op. cit.*). The seismic data indicate that these structures are controlled by listric thrust-faults that have an imbricate-fan geometry. Minor displacements affect the boundary between the non-reflective and reflective sedimentary layers in the upper 1 s of the data. The Dawson Fold Zone consists of tightly folded Upper Permian sedimentary rocks. Because of the steep dips, reflectivity is low, but faults with moderate easterly dips occur, and are best seen at the eastern end of line BMR89.B01 (Fig. 23). The major east-dipping detachment defines the base of this zone.

(Continued at foot of next page)

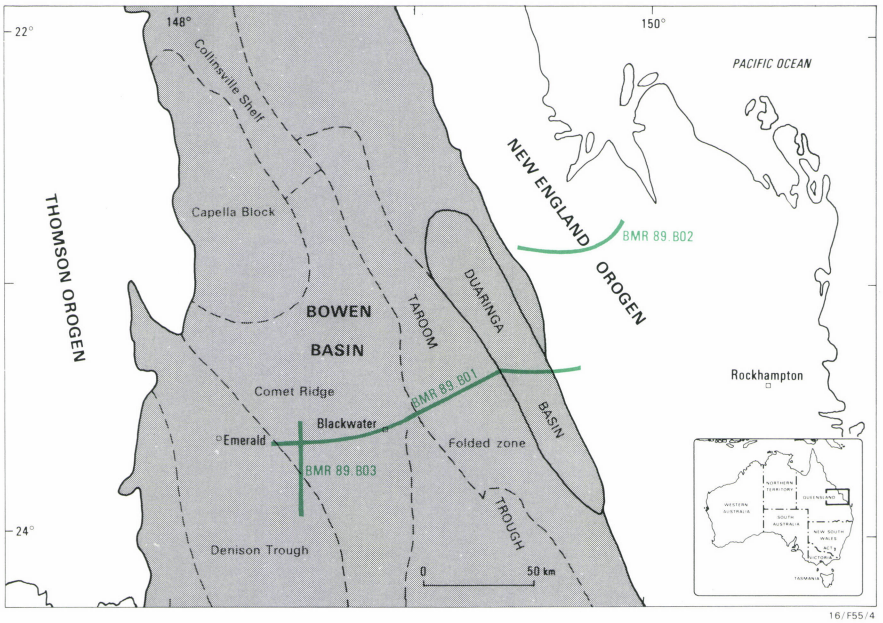

Fig. 22. Locations of the 1989 BMR deep seismic reflection survey lines in the Bowen Basin.

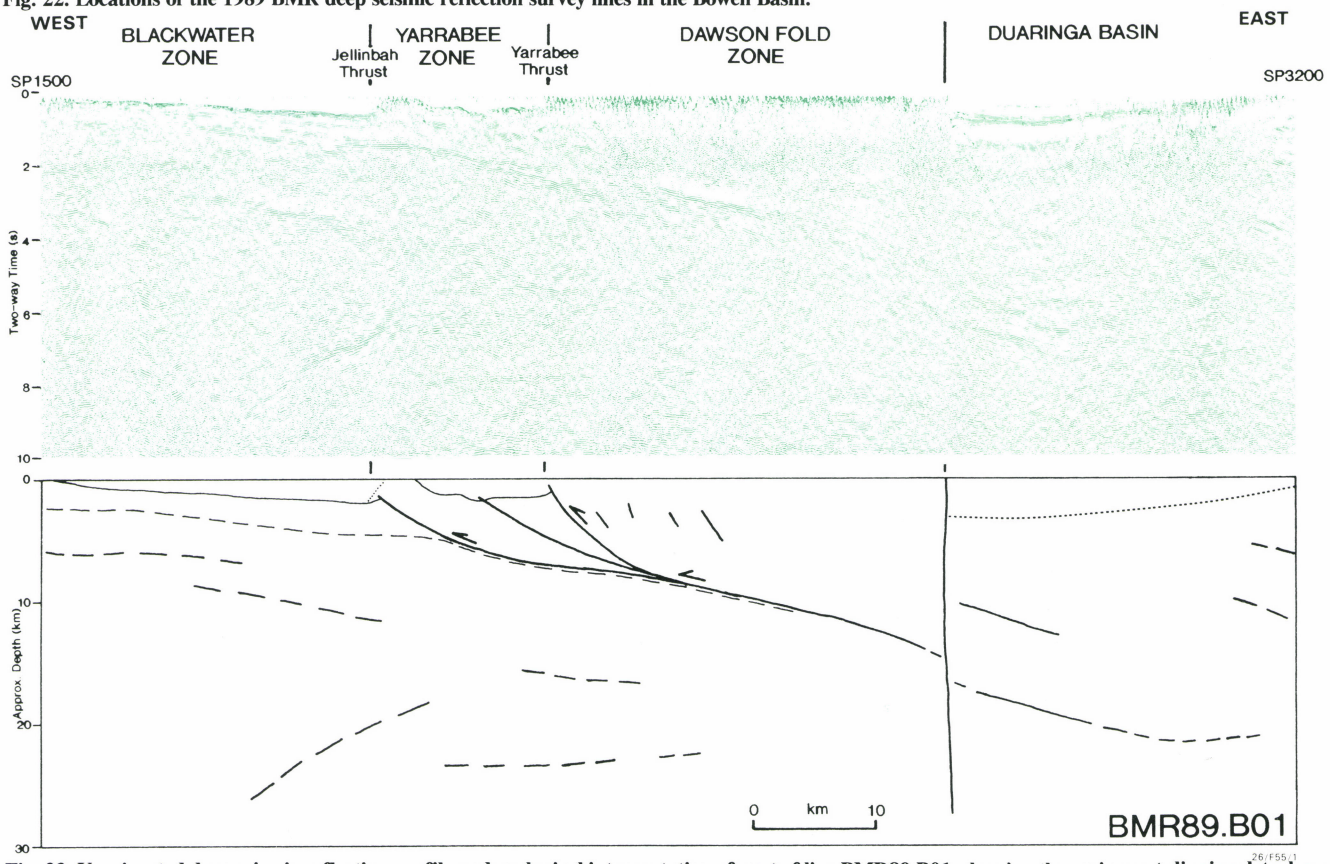

Fig. 23. Unmigrated deep seismic reflection profile and geological interpretation of part of line BMR89.B01, showing the major east-dipping detachment. Vertical scale equals horizontal scale for a velocity of 6 km s^{-1}.

New stable-isotope facility

BMR is currently negotiating to purchase new mass-spectrometry equipment for geochemical studies. The equipment will be used for high-sensitivity, high-precision ratio measurements on carbon, oxygen, sulphur, and hydrogen isotopes.

The new equipment will supplement the present VG-SIRA mass spectrometer which was purchased in 1983, and will enable us to study the isotopic compositions of materials which are available in only trace amounts. These materials include microscopic diamonds, microsamples of carbonate minerals and microfossils, and traces of sulphate and sulphide present in carbonate matrices and sediment pore-waters. The equipment will also enhance our capacity to accurately analyse minerals and groundwaters. An important new provision is the capacity to measure the isotopic compositions of individual organic compounds, such as biomarker hydrocarbons and the hydrocarbons of natural gas and petroleum condensates. To our knowledge, this facility will be unique in Australia.

The instrument will consist of a high-precision isotope-ratio mass spectrometer, microsample inlet system, mult-port automatic inlet system for batches of gas samples, and a gas-chromatograph inlet system with high-temperature combustion interface. This latter device separates complex mixtures of hydrocarbons into their individual components, combusts them, and analyses the resulting CO_2 stream for its ^{13}C content.

Isotope measurements on bulk saturate and aromatic hydrocarbon fractions of crudes is a very rough means of correlating oils with their putative source rocks or assigning marine *versus* terrestrial origins to oils. With the new equipment, a much higher degree of precision will be possible because the comparisons will be made on numerous individual components. For the first time, we shall be able to establish reliable source and maturity information on natural gases and condensates through isotopic means. This is because cracking of larger liquid hydrocarbons into gaseous molecules is accompanied by a kinetic isotope effect, so that starting isotopic signatures (close to those in the source bitumen) are shifted systematically as a function of maturity.

Isotopic measurement made at the molecular level promises to revolutionise many aspects of organic geochemistry as well as a range of biochemical and environmental studies. An example of how the new equipment can be used on an Australian hydrocarbon sample is shown in Figure 24. These hydrocarbons have been isolated from a modern microbial community, and represent a 'pristine' biological mixture unaffected by contamination from fossil-fuel sources. One of the most interesting and unexpected results to appear in this analysis is the degree to which the assemblage is isotopically heterogeneous. A 20‰ spread in the values is much greater than anticipated, and points to a variety of controls on fractionation. This is invisible when one looks at the isotopic composition of total organic carbon (-12 ‰ PDB) or total hydrocarbons — in this case about -15‰ PDB.

Points of interest in the data are that:

- the signatures are diverse (-8.8 to -27.7‰ PDB); TOC ^{13}C = -12‰; and the carbon source from which most were synthesised (bicarbonate in the water column above the community) is approximately +3‰ PDB;
- signatures of the highly branched C_{20} and C_{25} isoprenoid hydrocarbons are relatively heavy (ca. -11.4 and -12.8‰) and these are probably derived from *algal source* organisms, possibly ones also making the $C_{29:2}$ steroid (-12.8‰);
- the *cyanobacterial* (n-17:1) hydrocarbon biomarker is very light (-24.6‰);
- *cyanobacterial and bacterial* hopanoid hydrocarbons are light (-20 to -25‰);
- n-alkanes have multiple sources; the shorter (and heavy ones -20.8 to -21.4‰) probably arise from algal sources within the community, and are mixed with the odd-carbon-number predominant waxy alkanes (C_{25}-C_{31}, -26.1‰ to -27.7‰) from *terrestrial higher plant* inputs. These probably enter the mat via aeolian transport on dust particles. Their isotopic compositions are close to cuticular wax hydrocarbons isolated from the surrounding vegetation.

In this simple example, the foreign (land plant) signal is readily distinguished from the indigenous signals of the algal and bacterial hydrocarbons. It illustrates how the variety of individual sources of organic matter may be delineated when isotopic information is combined with chemical-structure information. The technique will be invaluable for environmental applications, and may enable the dissolved organic components of groundwater to be used as markers. In petroleum-related studies, biogenic and thermogenic gases will be distinguishable.

Further information can be obtained from Dr R.E. Summons or Mr Z. Roksandic (Onshore Sedimentary & Petroleum Geology Program) at BMR.

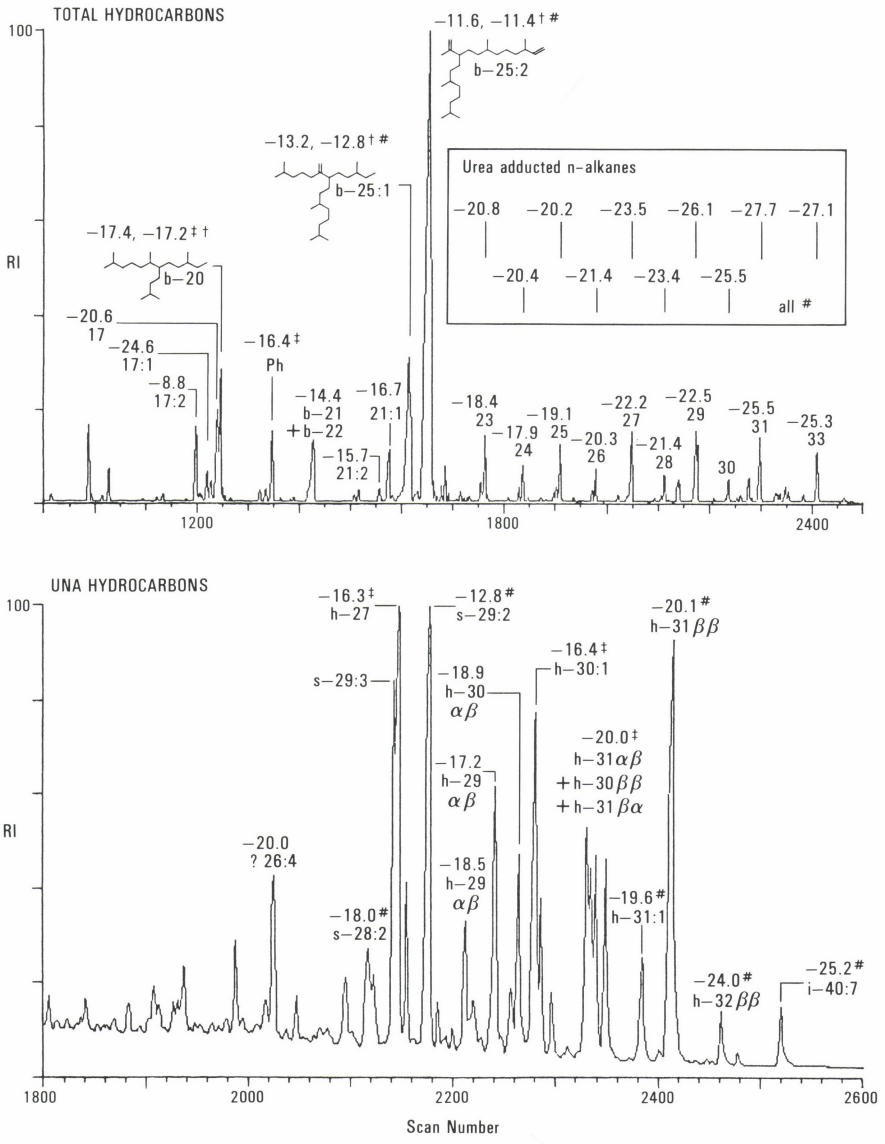

‡ *Incompletely resolved components* † *Duplicate analyses* # *Denotes peak without impurities*

Fig. 24. Gas chromatogram — derived from mass-spectrometry equipment identical with that which BMR is negotiating to buy — showing carbon-isotopic composition of hydrocarbons in a microbial mat community from Hamelin Pool, Shark Bay (WA). The gas-chromatogram elution profile has been annotated to show the identity and isotopic compositions of specific hydrocarbons from the microbial mat community. The abbreviations above each peak are the isotope composition (δ ^{13}‰ PDB) and a shorthand identification of the molecule's structure. Ph = phytane, b = highly branched isoprenoid, s = steroid, h = hopanoid together with the number of carbon atoms in the molecule. n-Alkanes just have their carbon number, and the boxed inset shows signatures for the n-alkanes after they were isolated from the mixture as a urea adduct. The adducted hydrocarbons are thus unaffected by co-eluting branched and cyclic components and vice versa.

Bowen Basin

(Continued from previous page)

In the eastern part of line BMR89.B01, the overlying Tertiary oil-shale-bearing Duaringa Basin has a pronounced asymmetric geometry, which was possibly controlled by movement along a subvertical strike-slip fault (Fig. 23) — that is, the basin is probably transtensional in origin. The upper oil shale unit is too shallow to be detected in the seismic data. The central claystone unit is relatively non-reflective, in marked contrast to the highly reflective character of the lower oil shale unit.

For further information, contact Kevin Wake-Dyster, David Johnstone, or Russell Korsch (Onshore Sedimentary & Petroleum Geology Program) at BMR.

Petroleum source-rock assessment

(Continued from back page)

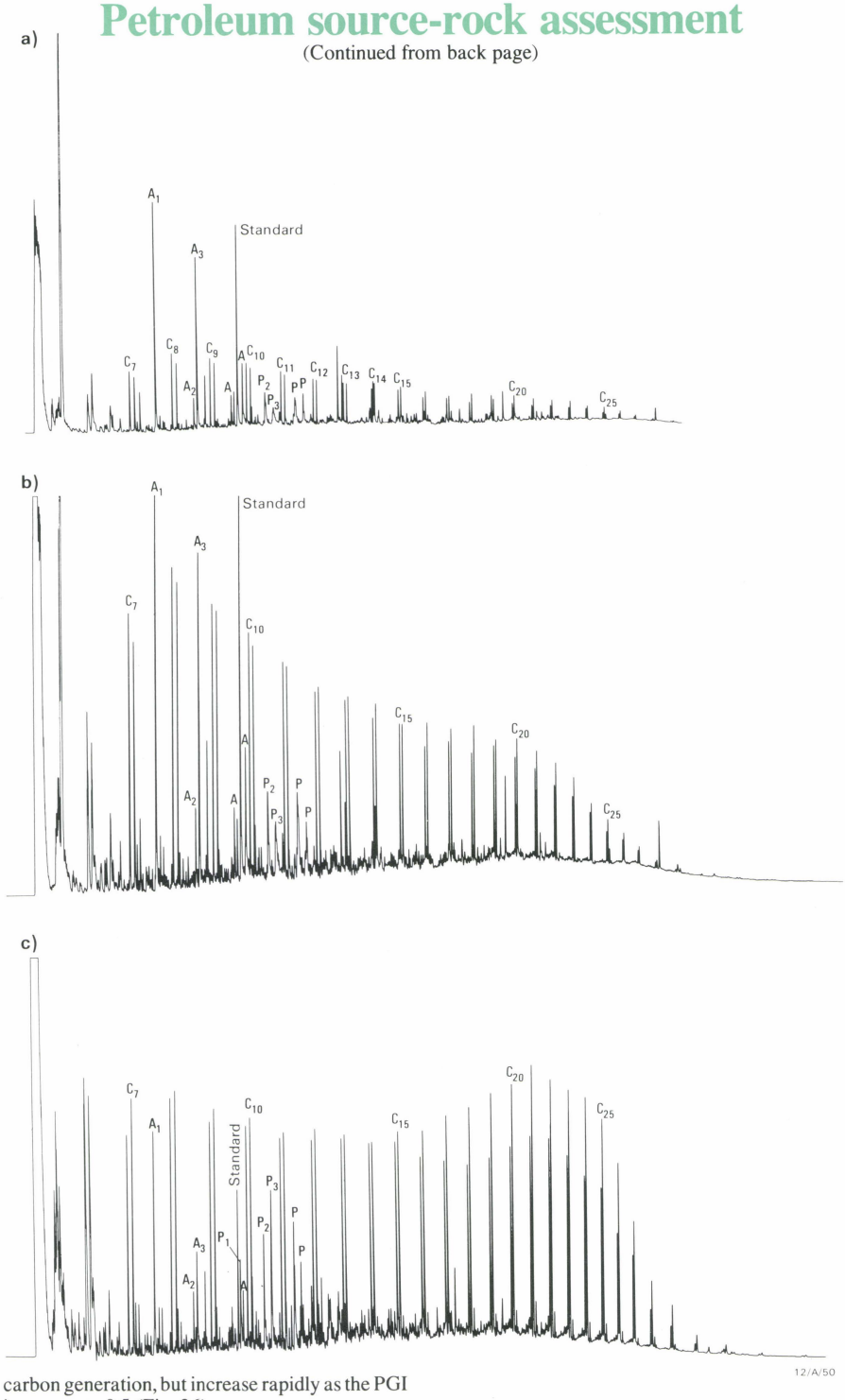

Fig. 25. Representative pyrolysis gas chromatograms: A, Permian sample showing dominance of low-molecular-weight aromatics and phenols over normal hydrocarbons; B,Permian sample showing abundant low-molecular-weight normal hydrocarbons; C, Tertiary sample showing abundant high-molecular-weight normal hydrocarbons. Peak identifications: C_7-C_{27}, alk-1-enes/alkanes; aromatics, A-A_3; phenols, P-P_3.

carbon generation, but increase rapidly as the PGI increases to 0.5 (Fig. 26).

Once kerogen cracking commences, hydrocarbon generation is extremely rapid (Fig. 26) and the bulk of oil generation occurs in the reflectance range 0.8 to 1.0% Ro. As a result the zone of effective oil generation and migration is extremely narrow. This is consistent with the paraffinic nature of the hydrocarbon product and the relatively narrow range of bond energies in normal hydrocarbon precursors. It suggests that the component of the terrestrial organic matter that is actually generating liquid hydrocarbons is equivalent to a type I kerogen — i.e., an aliphatic biopolymer analogous to that recently found in plant cuticles and bark. During the early stages of hydrocarbon generation, expulsion is relatively inefficient; at a PGI of 0.16 the expulsion efficiency is 25%, and rises to 75% at a PGI of 0.5 (Fig. 26). This reflects the importance of a high hydrocarbon saturation in primary migration, and emphasises that oil expulsion will be more efficient in richer source rocks. The Walloon coals are oil-prone, and hence begin to generate hydrocarbons at a lower level of maturation than the gas-prone Westphalian coals of Europe. However, at high maturation levels the Walloon coals behave more like these gas-prone coals in general, and the increase in petroleum expulsion efficiency to 90% reflects the efficiency of gas migration.

The Rock Eval measurement does not discriminate between oil and gas potential. An unresolved question therefore has been the relative proportions of oil *versus* gas that are generated during the main phase of oil generation in terrestrial sequences. The remaining gas potential at any stage of maturation can be determined by measuring the yield of C_1-C_5 hydrocarbons by pyrolyis gas chromatography, as described above. Measurements of likely gas-to-oil ratios for the residual petroleum potential of selected Walloon coals are displayed on the PGI curve in Figure 26. The gas-to-oil ratio of the pyrolysable hydrocarbons does not show a significant change up to a vitrinite reflectance of 1.0%, indicating that the petroleum generated in the oil window has a fixed oil-to-gas ratio. Only when extensive cracking occurs above 1.0% Ro does the gas-to-oil ratio change.

Permian coals. Preliminary calculations of PGI and PEE for samples from the Cooper Basin (Fig. 26) show a slightly different pattern of behaviour. Hydrocarbon generation patterns are initially similar to the Walloon coals, but at a PGI ratio of about 0.4 the petroleum generation curve trends to the gas generation line defined by the Westphalian coals. These results clearly show the lower oil potential of the Cooper Basin source rocks. The petroleum expulsion efficiencies are correspondingly higher for a given PGI and maturation level, reflecting probable higher gas-to-oil ratios of the generated products and the relative efficiency of migration in the gas phase compared with the liquid phase. These results tend to support previous suggestions that migration can occur from non-marine source rocks at lower thresholds of liquid hydrocarbon concentrations because of the presence of cogenerated gas. Gas-to-oil ratios in combination with absolute concentrations are therefore required to understand the timing of petroleum migration from non-marine source rocks.

For further information, contact Dr Trevor Powell or Dr Chris Boreham (Onshore Sedimentary & Petroleum Geology Program) at BMR.

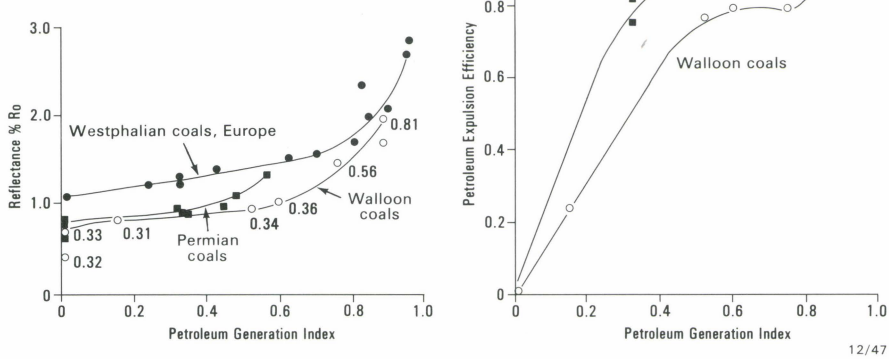

Fig. 26. Evolution of Petroleum Generation Index and Petroleum Expulsion Efficiency with maturation in the Walloon Coal Measures, Clarence-Moreton Basin, and Permian coals in the Cooper Basin. Numbers denote ratio of C_1-C_5 hydrocarbons to C_6-C_{27} normal hydrocarbons (gas-to-oil ratio) of residual oil potential in selected samples from the Walloon coals as determined by pyrolysis gas chromatography. Data for Westphalian coals is derived from Cooles & others (1986).

Petroleum source-rock assessment and hydrocarbon generation in terrigenous sequences

Considerable uncertainty and argument have focused on the recognition of non-marine source rocks and the timing of hydrocarbon generation in terrigenous sequences. Systematic studies, by BMR, of Permian through Tertiary coals and carbonaceous shales using pyrolysis techniques, in conjunction with conventional petrographic and bulk geochemical measurements, have resolved many of the ambiguities in geochemical and petrographic relationships. The results facilitate a more rigorous assessment of source-rock quality, and allow quantitative aspects of petroleum generation and migration to be considered in terrigenous source rocks.

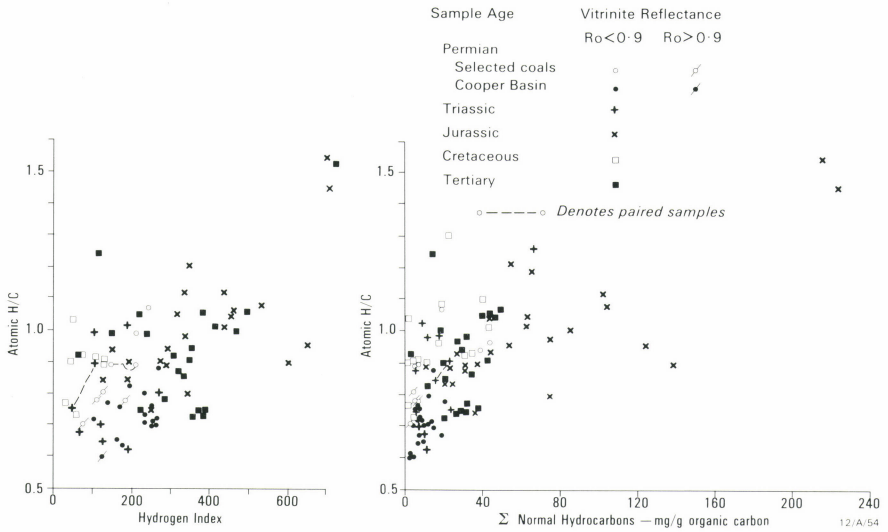

Fig. 27. Variation in pyrolysable hydrocarbon yield with atomic H/C ratio of kerogen; A, Hydrogen Indices from Rock Eval pyrolysis; B, normal hydrocarbons (C_7-C_{27}) from pyrolysis gas chromatography.

Theoretical considerations suggest that the hydrocarbon potential of terrigenous organic matter should be explicable in terms of the relative proportions of hydrogen-poor and hydrogen-rich components represented by the coal macerals inertinite plus vitrinite and liptinite respectively. A systematic study of coals and carbonaceous shales ranging in age from Permian to Tertiary has shown a poor relationship between the bulk geochemical measurements such as elemental analysis and pyrolytic hydrocarbon yield (Rock Eval; Fig. 27), and between these geochemical measurements and petrographic composition. This contrasts with rich potential marine and lacustrine source rocks.

Because terrigenous oils are mainly paraffinic, quantitative measurement of the yield of C_7-C_{30} normal hydrocarbons by pyrolysis gas chromatography can be used as a direct measure of the ability of non-marine organic matter to yield paraffinic oil (Fig. 25). Utilisation of this technique removes many of the ambiguities associated with subjective interpretation of petrographic data and bulk geochemical measurements, and allows more confident interpretation of the results of these widely used techniques. This procedure has been applied, in conjunction with petrographic and bulk geochemical measurements, to the systematic study of the Permian to Tertiary samples from the Cooper, Eromanga, Clarence-Moreton, and Gippsland Basins — with the following results.

Source-rock assessment

Terrigenous organic matter ranging in age from Permian to Tertiary can contain normal hydrocarbon structures capable of producing paraffinic oils. For most terrestrial kerogens, this capability is not simply related to gross elemental composition (Fig. 27). Below an atomic H/C ratio of 1.0, atomic H/C ratios of terrigenous organic matter are largely controlled by the degree of carbonisation and not the content of paraffinic components. Nevertheless, paraffinic components may occur in kerogen even when the atomic H/C ratio may be relatively low (0.7), and the organic matter can produce normal hydrocarbons on pyrolysis.

Below Hydrogen Indices of 300, Rock Eval analysis is not a good indicator of the ability of coals and carbonaceous shales to yield paraffinic hydrocarbons. There is a broad range in the yields of normal hydrocarbons from flash pyrolysis for a given Hydrogen Index below 300, and vice versa.

Liptinite-poor (<10%) samples may yield significant amounts of hydrocarbons, but typically these have a low wax yield (normal hydrocarbons above C_{17}). Liptinite-rich samples with abundant sporinite and liptodetrinite macerals give lower yields of normal hydrocarbons, and these are mainly of lower molecular weights. The macerals suberinite and to a lesser extent cutinite are associated with high yields of waxy hydrocarbons, but some samples with high yields of waxy hydrocarbons do contain large amounts of these macerals.

These results clearly show that there is no simple relationship between maceral composition and hydrocarbon potential. Reconnaissance geochemical or petrographic techniques must be supported by a judicious application of pyrolysis gas-chromatographic techniques for quantitative assessment of non-marine source rocks. For adequate petrographic assessment, the relative abundance of the different liptinite macerals is absolutely necessary, and subdivision of the vitrinite group is probably desirable.

Hydrocarbon generation

The maturation level and timing of hydrocarbon generation has also been the subject of considerable controversy. Oil generation and migration have been postulated to occur at maturities varying from 0.5% Ro (vitrinite reflectance) to 1.0% Ro. The abundance of data collected in our study of the Clarence-Moreton Basin, and the apparent uniformity of organic matter in the Walloon Coal Measures, have enabled us to calculate the amounts of hydrocarbons generated, and the relative timing of hydrocarbon generation and expulsion, by applying the approach of Cooles & others (1986: *Organic Geochemistry*, **10**, 235-246). Rock Eval data are used to calculate the Petroleum Generation Index (PGI) and the Petroleum Expulsion Efficiency (PEE):

$$\text{PGI} \equiv \frac{\text{Petroleum generated} + \text{Initial petroleum}}{\text{Total petroleum potential}}$$

$$\text{PEE} \equiv \frac{\text{Petroleum expelled}}{\text{Petroleum generated} + \text{Initial petroleum}}$$

Walloon coals. A plot of PGI *versus* vitrinite reflectance (Fig. 26) shows that the Walloon Coal Measures do not begin to generate significant amounts of hydrocarbons until a vitrinite reflectance level of 0.75% Ro. Comparison of the theoretical hydrocarbon yields with those actually measured on individual samples shows that there are changes in hydrocarbon yield and composition that precede the main phase of hydrocarbon generation as measured by PGI. Examination of gas chromatograms of samples from this interval show that the hydrocarbons retain their immature aspect. This is probably attributable to the formation of hydrocarbons from free fatty acids, esters, and alcohols before the main phase of kerogen cracking. This process is quantitatively much less significant, and is not accounted for by the calculation of PGI, which is based on changes in pyrolysis yields of kerogen. Petroleum expulsion efficiencies are low during these initial stages of hydro-

(Continued on reverse of this page.)

BUREAU OF MINERAL RESOURCES, GEOLOGY AND GEOPHYSICS
Cnr Constitution Avenue and Anzac Parade, Canberra, ACT

Postal Address: GPO Box 378, Canberra, ACT 2601
Telephone: (06) 249 9111 *Telex:* 62109 *Fax:* (06) 248 8178
Executive Director: Professor R.W.R. Rutland AO

This number of the *BMR Research Newsletter* was edited by G.M. Bladon and word-processed by E. Robinson; the figures were drawn by the staff of BMR's Cartographic Services Unit

The twice-yearly *BMR Research Newsletter* is designed to provide the geoscientific community with early information on the progress of research and on the availability of new data resulting from the implementation of the BMR Programs; to provide commentaries on relevant research developments worldwide; and to encourage close liaison between BMR and the community. Readers' comments and suggestions — addressed to the Executive Director — are welcome. Requests to be placed on the mailing list should be addressed to: Information Section, Bureau of Mineral Resources, GPO Box 378, Canberra, ACT 2601.